Numerically Optimized Diabatic Distillation Columns

von der Fakultät für Naturwissenschaften
der Technischen Universität Chemnitz
genehmigte Dissertation zur Erlangung des akademischen Grades

doctor rerum naturalium

(Dr. rer. nat.)

vorgelegt von Dipl.-Ing. Markus Schaller
geboren am 19. Juni 1973 in Vorau (Österreich)

eingereicht am 4. Mai 2007

Gutachter: Prof. Dr. Karl Heinz Hoffmann (TU Chemnitz)
Prof. Dr. Michael Schreiber (TU Chemnitz)
Prof. Dr. Peter Salamon (San Diego State University)

Tag der Verteidigung: 10. Juli 2007

Bibliographische Beschreibung

Schaller, Markus
Numerically Optimized Diabatic Distillation Columns
Technische Universität Chemnitz, Fakultät für Naturwissenschaften, 2007
Dissertation (in englischer Sprache)
86 Seiten, 35 Abbildungen, 2 Tabellen, 57 Literaturzitate

Referat

Im Gegensatz zur konventionellen adiabatischen Destillation erfolgt bei der diabatischen Destillation Wärmeaustausch nicht nur am Kondensator und Verdampfer, sondern auch innerhalb der Kolonne an den einzelnen Siebböden, was die Entropieproduktion (=Exergieverlust) des Destillationsprozesses stark reduziert. In dieser Arbeit werden Modellsysteme zur diabatischen Destillation von idealen binären Gemischen mittels numerischer Optimierung untersucht.

Das Ausgangsmodell beschränkt sich auf die Minimierung der Entropieproduktion verursacht durch Wärme- und Massentransport im Inneren der diabatischen Destillationskolonne. Im zweiten Modell wird das diabatische Modell um die Irreversibilität bedingt durch den Wärmeaustausch mit der Umgebung erweitert. Im dritten Modellsystem wird anstelle der bis dahin voneinander unabhängig geregelten Bodentemperaturen eine diabatische Implementierung mit seriellen Wärmetauschern untersucht, die nur mehr vier Kontrollvariablen besitzt und besonders zur praktischen Anwendung geeignet ist.

Für alle diabatischen Modelle werden die minimale Entropieproduktion und optimalen Betriebsprofile numerisch ermittelt, und mit konventionellen Destillationskolonnen verglichen. Alle Ergebnisse zeigen eine deutlich Reduktion der Entropieproduktion für den diabatische Fall, besonders bei Kolonnen mit vielen Böden.

Schlagwörter

Binäres Gemisch, Destillationskolonne, Diabatische Destillation, Entropieproduktion, Equal Thermodynamic Distance, Exergie, Irreversibilität, Nichtgleichgewichtsthermodynamik, Optimierung, Wärmeaustauscher

Contents

Chapter 1

Introduction

A major application of thermodynamics is the provision of in-principle performance bounds for any kind of energy conversion process. The oldest and most prominent of such performance limits is the Carnot efficiency giving the maximum efficiency of any reversible heat engine working between two infinite heat reservoirs. Much later, in the second half of the 20th century, when the oil crisis of the 1970s required a stronger awareness of limited energy resources, performance limits have been extended to thermodynamic processes subject to finite time or finite rate constraints. Among such studies, the Curzon-Alborn-Novikov efficiency [1] is a remarkable result and early milestone of this emerging thermodynamic research area, which is known as finite-time thermodynamics [2, 3] or, more general, as control thermodynamics [4].

Naturally, such problems lead to the use of mathematical optimization. A performance objective is optimized subject to constraints imposed by the thermodynamic process under consideration. As a result, the optimal controls of the process are determined that achieve the optimal value of the objective. Weaker, but generally more tractable is the question for bounds on the optimal values of the objective. Hence, several ways to simplify and generalize problems in control thermodynamics have been proposed. Salamon [4] categorizes them into principles of problem simplification, principles related to maximum power, and principles related to minimum entropy production. With the help of such principles, one can find performance bounds for a particular class of thermodynamic processes aside from design details or other engineering aspects. Furthermore, such generalized models are an orientation and starting point for more detailed further analyes, e. g. numerical investigations. A mentionable successful tool in this context is the

concept of endoreversibility [5–10], where all irreversibilities are located at the couplings of an reversible subsystem to its surroundings.

There has been plenty of research activity in the field of control thermodynamics during the last decades. Many publications focus on the power or efficiency optimization of all kinds of heat engines (e.g. [11–13]), or the minimization of entropy production in thermal engineering processes [14, 15]. Solar energy conversion has been investigated [16, 17], and we also find early control thermodynamics approaches to chemical processes [18, 19] and distillation [20]. In this thesis we focus on the optimization of the latter.

Distillation

In many chemical production processes raw materials or end products are given as liquid mixtures which have to be separated into their components. Fractional distillation is the most important method used for the separation of liquid mixtures or liquified gaseous mixtures. Among numerous industrial applications, distillation is particularly important for the petrochemical industry. In oil refineries, crude oil is distilled to yield various commercial oil products.

Since distillation is a heat driven separation process, it significantly contributes to the energy consumption. In the USA about 10% of the industrial energy consumption accounts for distillation [21, 22]. More than 70% of the operation costs are caused by the energy expenses [23]. But the second-law efficiency of conventional distillation is very low, only around 5–20% [24, 25]. This means that distillation is associated with a high entropy production (= exergy loss) and hence degradation of energy. To reduce the exergy wasted it is recommended to alter design and operation of the distillation process. This is achieved by spreading the heat requirements over the whole length of a distillation column. Such design consideration is referred to as *diabatic* distillation.

This document presents a numerical investigation of diabatic distillation models with emphasis on the determination of minimum entropy production and the corresponding optimal operating characteristics.

Document Structure

Chapter 2 introduces the concept of diabatic distillation which allows enormous reduction of the entropy production compared to conventionally de-

signed distillation columns. A mathematical model for diabatic tray distillation is systematically built up for ideal binary mixtures. From this model expressions for the heating profile and total entropy production are obtained as functions of the temperature profile inside the distillation column. For further comparison, the asymptotic theory of equal thermodynmic distance (ETD) is outlined.

In Chapter 3 the entropy production in a diabatic distillation column is minimized by applying Powell's algorithm to the temperature profile inside the distillation column. From the optimal temperature profile the minimal total entropy production is obtained and compared to the entropy production prescribed by the ETD theory and to the entropy production of a conventional column. The comparisons are performed for columns of different length and for different purity requirements. Additionally, the temperature profiles, the heating requirements for each tray and the entropy production per tray are evaluated for numerically optimized, conventional and ETD columns.

In Chapter 4 the distillation model is extended to include the heat transfer irreversibilies arising from the heat coupling of the column to the surroundings. Two different heat transfer laws, Newton's linear law and Fourier's inverse law are investigated. For both heat transfer laws the minimum total entropy production is determined by numerical optimization for varying heat resistance. For three column lengths, the optimal operation profiles (heat requirements and entropy production per tray) are computed for low, high and industrially relevant values of heat resistance.

In Chaper 5 the concept of independently adjustable tray temperatures is replaced by a heat exchanger installation that only requires four control variables. For a sample column with this particular design, the optimal operation profiles are determined and compared to a conventional column. Furthermore we focus on how much more irreversibility one must pay for the reduction of control variables.

Chapter 6 summarizes the core results of this thesis and gives an outlook on potential open questions for further research.

Chapter 2

The Concept of Diabatic Distillation

Distillation makes use of the differences in volatility of the components of a mixture. The more volatile component has the lower boiling temperature. Hence, when the liquid mixture is heated up to its boiling temperature, the resulting vapor is enriched with the more volatile component. After condensing this vapor one obtains a liquid with a higher concentration of that component. This process is repeated until the components are separated into specified purities.

Fractional distillation is performed in vertical columns divided into trays. On each tray one stage of purification is carried out. The reboiler at the bottom serves as heat source, the condenser at the top serves as heat sink. According to the desired purity, heat Q_{B} is delivered to the bottom and heat Q_{D} is removed from the top. This creates a temperature gradient decreasing vertically along the column. The feed flow F carrying the mixture to be separated is introduced near the middle of the column. On each tray, the mixture boils resulting in vapor entering the tray above. The tray has an overflow tube permitting the liquid to flow to the tray below. The more volatile component of the binary mixture is removed at the top as distillate D, the other is removed at the bottom as bottom product B (see figure 2.1, on the left).

The thermodynamic inefficiency of conventional distillation has the following reason: heat is added only at the highest temperature T_{B} in the column, while the heat removal takes place only at the lowest temperature T_{D} in the column. Hence, the energy is degraded over the whole teperature range $T_{\mathrm{B}} - T_{\mathrm{D}}$ of the column. This is the reason for the high entropy production associated

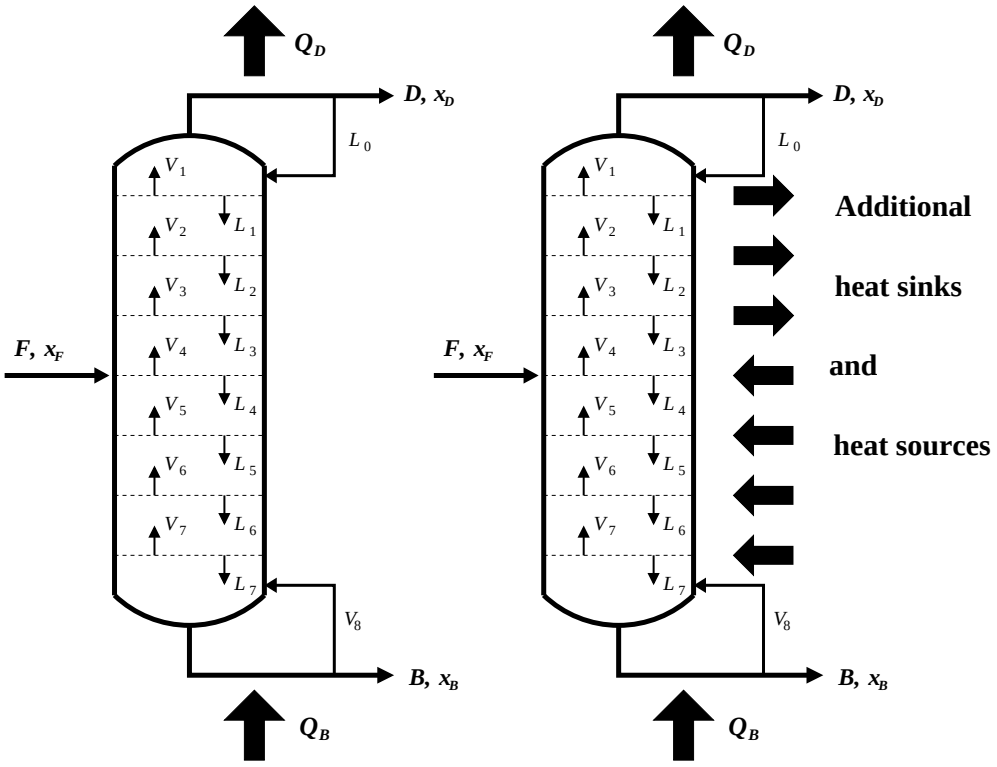

Figure 2.1: Sketch of a conventional adiabatic distillation column and a diabatic column with additional heat exchange. Both columns have $N = 8$ trays including the reboiler as tray 8. The L's and V's denote the liquid and vapor flows, respectively.

with distillation.

From that it can be concluded that a redistribution of the heat requirements over the whole length of the column will result in a lower entropy production [26]. Then most of the heat would be used over a smaller temperature range than $T_\mathrm{B} - T_\mathrm{D}$ [27]. A column designed in such a way is referred to completely diabatic distillation column because heat exchange between column and surroundings occurs on each tray of the column (figure 2.1, on the right). Other terms than diabatic used in literature are 'thermally controlled' or 'heat intergrated' column. The idea goes back to the work of Fonyo [28, 29] in the early 1970s but recently has been explored by Rivero [30–32], Salamon, Nulton and Andresen [22, 27], and Kjelstrup, Sauar, and De Koeijer [24, 25, 33–36].

Now, the interesting question is how to determine the optimal temperature and heating profiles ensuring operation at minimum entropy production. Various theoretical approaches exist to estimate optimal performance

of diabatic distillation columns, but so far there is only one systematic experimental study done by Rivero [30]. Salamon, Andresen and Nulton [22, 27] use a thermodynamic metric based on the entropy state function of the considered mixture, which leads to the theory of equal thermodynamic distance (ETD). Kjelstrup *et al.* [25, 33, 34] use a method that is based on Onsager's irreversible thermodynamics, in which the entropy production is represented in terms of thermodynamic forces and fluxes. From this theory the principle of equipartition of thermodynamic forces (also called isoforce principle) is derived [37, 38]. Tondeur and Kvaalen [39] suggest a different equipartition principle as optimality criterion, the equipartition of entropy production. For summaries and general discussions on equipartition principles in thermodynamics the reader should refer to [4, 40, 41].

Because of the additional heat exchangers, the investment costs for a diabatic column are significantly higher than for a conventional one. So-called partially diabatic columns are considered to allow a trade-off between extra equipment costs and minimizing entropy production. In these columns only selected trays are thermally controlled. For example, De Koeijer *et al.* use the isoforce principle to find optimal locations of the trays to be heated or cooled [24]. However, this thesis only considers fully diabatic columns, because they give the ultimate limit of what is possible in reducing the entropy production.

Each of these theoretical approaches bases on a particular thermodynamic principle which gives an approximation to the optimum. To assess the validity of these approximations, numerical minimization has shown to be very effective [35, 42]. Before introducing a fully numerical optimization scheme in the next chapter, a mathematical model for binary distillation is presented here.

2.1 Model Description

The distillation column is considered to be operating at steady-state so all extensive quantities are per unit time. For convenience, only binary mixtures are considered and the pressure is assumed to be constant throughout the column.

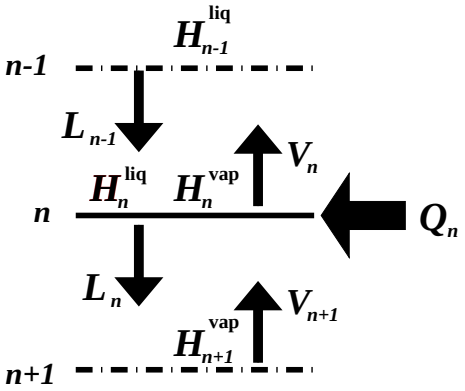

Figure 2.2: Definitions of quantities around tray n appearing in the balance equations (2.3), (2.4) and (2.8).

2.1.1 Material Balance

In steady state operation, the feed, distillate and bottoms obey the flow balance equations

$$F = D + B, \tag{2.1}$$
$$x_{\mathrm{F}} F = x_{\mathrm{D}} D + x_{\mathrm{B}} B, \tag{2.2}$$

where x_{F}, x_{B} and x_{D} denote the corresponding mole fractions of the more volatile component (lower boiling point) in the liquid phase. Similarly, the amount of material flowing out of a tray must be equal to the amount of material flowing into a tray. Hence, vapor coming up from tray $n+1$ and liquid flowing down from tray n have to balance the distillate D above the feed and the bottoms B below the feed respectively (see figure 2.2),

$$V_{n+1} - L_n = \begin{cases} D & \text{above feed} \\ -B & \text{below feed} \end{cases}, \tag{2.3}$$

$$y_{n+1} V_{n+1} - x_n L_n = \begin{cases} x_{\mathrm{D}} D & \text{above feed} \\ -x_{\mathrm{B}} B & \text{below feed} \end{cases}. \tag{2.4}$$

On the uppermost tray ($n = 1$) the balance equations simplify to $V_1 = D + L_0$ and $y_1 = x_{\mathrm{D}}$; for the lowest tray ($n = N$, the reboiler) one obtains $L_N = B$ and $x_N = x_{\mathrm{B}}$. For our purposes of looking for optimal diabatic columns, the reflux L_0 is taken equal to zero. Its purpose in an adiabatic column is to help carry heat out of the column. This function is not needed in the diabatic column since heat can be taken directly from tray one.

2.1.2 Equilibrium State Equations

It is assumed that each tray is in thermodynamic equilibrium. The temperature dependencies of the molar fractions x and y in the liquid and vapor phase respectively, are given by the state equations for an ideal solution model [43]

$$y = x \exp\left[\frac{\Delta H^{\mathrm{vap},1}(T)}{R}\left(\frac{1}{T_{\mathrm{b},1}} - \frac{1}{T}\right)\right], \tag{2.5}$$

$$1 - y = (1 - x) \exp\left[\frac{\Delta H^{\mathrm{vap},2}(T)}{R}\left(\frac{1}{T_{\mathrm{b},2}} - \frac{1}{T}\right)\right]. \tag{2.6}$$

Here $T_{\mathrm{b},1}$ and $T_{\mathrm{b},2}$ denote the boiling points of the two pure components. The enthalpy differences $\Delta H^{\mathrm{vap},1}(T)$ and $\Delta H^{\mathrm{vap},2}(T)$ are calculated as

$$\Delta H^{\mathrm{vap},i}(T) = \Delta H_b^{\mathrm{vap},i} + (T - T_{\mathrm{b},i})(c_{\mathrm{p}}^{\mathrm{vap},i} - c_{\mathrm{p}}^{\mathrm{liq},i}), \qquad (i = 1, 2) \tag{2.7}$$

where $\Delta H_b^{\mathrm{vap},i}$ are the heats of vaporization of the pure components and $c_{\mathrm{p}}^{\mathrm{liq},i}$ and $c_{\mathrm{p}}^{\mathrm{vap},i}$ are the corresponding heat capacities. Equation (2.7) requires the heat capacities to be temperature independent.

2.1.3 Heat Balance

In order to calculate the heat required at each tray to maintain the desired temperature profile, the energy balance has to be maintained for each tray n:

$$Q_n = V_n H_n^{\mathrm{vap}} + L_n H_n^{\mathrm{liq}} - V_{n+1} H_{n+1}^{\mathrm{vap}} - L_{n-1} H_{n-1}^{\mathrm{liq}}. \tag{2.8}$$

For conventional adiabatic distillation columns, equation (2.8) would be equal to zero (for $1 \leq n < N$), and there would be no control parameters over which to optimize. The enthalpies H^{vap} and H^{liq} carried by the vapor and liquid flows are determined by

$$H^{\mathrm{liq}}(T) = x\, c_{\mathrm{p}}^{\mathrm{liq},1}(T - T_{\mathrm{ref}}) + (1 - x)\, c_{\mathrm{p}}^{\mathrm{liq},2}(T - T_{\mathrm{ref}}), \tag{2.9}$$

$$H^{\mathrm{vap}}(T) = y\left[c_{\mathrm{p}}^{\mathrm{liq},1}(T - T_{\mathrm{ref}}) + \Delta H^{\mathrm{vap},1}(T)\right] + \\ +(1 - y)\left[c_{\mathrm{p}}^{\mathrm{liq},2}(T - T_{\mathrm{ref}}) + \Delta H^{\mathrm{vap},2}(T)\right] \tag{2.10}$$

T_{ref} is an arbitrary reference temperature whose value drops out of the calculations. It represents the temperature at which the (relative) enthalpy of the pure liquid is zero. Here we assumed constant heat capacities and noninteracting mixture of ideal gases for the vapor phase.

For the lowest tray the energy balance reduces to

$$Q_N = V_N H_N^{\mathrm{vap}} + B H_N^{\mathrm{liq}} - L_{N-1} H_{N-1}^{\mathrm{liq}}. \tag{2.11}$$

For condenser and reboiler we obtain

$$\begin{aligned} Q_{\mathrm{D}} &= (D + L_0)(H^{\mathrm{vap}}(T_1) - H^{\mathrm{liq}}(T_{\mathrm{D}})), & (2.12)\\ Q_{\mathrm{B}} &= Q_N. & (2.13) \end{aligned}$$

For reflux $L_0 = 0$, equation (2.12) becomes

$$Q_{\mathrm{D}} = D(H^{\mathrm{vap}}(T_1) - H^{\mathrm{liq}}(T_{\mathrm{D}})), \tag{2.14}$$

while for the uppermost tray equation (2.8) turns into

$$Q_1 = D H_1^{\mathrm{vap}} + L_1 H_1^{\mathrm{liq}} - V_2 H_2^{\mathrm{vap}}. \tag{2.15}$$

On the feed tray n_{F}, the enthalpy of the feed flow has to be explicitely added in equation (2.8):

$$Q_{\mathrm{F}} = Q_{n_{\mathrm{F}}} - F H^{\mathrm{liq}}(T_{\mathrm{F}}). \tag{2.16}$$

Note that it is assumed that the feed enters as liquid at its boiling temperature T_F. The feed tray n_{F} is chosen such that the inequality $T_{n_{\mathrm{F}}-1} < T_{\mathrm{F}} < T_{n_{\mathrm{F}}}$ holds.

2.1.4 Entropy Production

Equations (2.1)–(2.16) allow us to evaluate the entropy production of the distillation process. The entropy production per tray can be determined from an entropy balance for each tray analogous to the heat balance (2.8). In order to focus on the separation process proper, unobscured by issues of heat exchange, we define our system to be the interior of the column. This makes the irreversibility associated with the heat transfer in and out of the column extraneous to the subsequent optimization. Hence, we take the source temperatures of the Q_n to be equal to the tray temperatures T_n. For the entropy production per tray one then obtains

$$\Delta S_n^{\mathrm{u}} = V_n s_n^{\mathrm{vap}} + L_n s_n^{\mathrm{liq}} - V_{n+1} s_{n+1}^{\mathrm{vap}} - L_{n-1} s_{n-1}^{\mathrm{liq}} - \frac{Q_n}{T_n}. \tag{2.17}$$

The s^{liq} and s^{vap} are the entropies per mole of liquid and vapor flow, respectively,

$$\begin{aligned} s^{\mathrm{liq}}(T) &= x\left[s_{\mathrm{ref},1} + c_{\mathrm{p}}^{\mathrm{liq},1}\ln\left(\frac{T}{T_{\mathrm{ref}}}\right)\right] + (1-x)\left[s_{\mathrm{ref},2} + c_{\mathrm{p}}^{\mathrm{liq},2}\ln\left(\frac{T}{T_{\mathrm{ref}}}\right)\right] - \\ &- R[x\ln x + (1-x)\ln(1-x)], \qquad (2.18) \\ s^{\mathrm{vap}}(T) &= y\left[s_{\mathrm{ref},1} + c_{\mathrm{p}}^{\mathrm{liq},1}\ln\left(\frac{T}{T_{\mathrm{ref}}}\right)\right] + (1-y)\left[s_{\mathrm{ref},2} + c_{\mathrm{p}}^{\mathrm{liq},2}\ln\left(\frac{T}{T_{\mathrm{ref}}}\right)\right] + \\ &+ y\left[\Delta H_{\mathrm{b}}^{\mathrm{vap},1} + (c_{\mathrm{p}}^{\mathrm{vap},1} - c_{\mathrm{p}}^{\mathrm{liq},1})\ln\left(\frac{T}{T_{\mathrm{b},1}}\right)\right] + \\ &+ (1-y)\left[\Delta H_{\mathrm{b}}^{\mathrm{vap},2} + (c_{\mathrm{p}}^{\mathrm{vap},2} - c_{\mathrm{p}}^{\mathrm{liq},2})\ln\left(\frac{T}{T_{\mathrm{b},2}}\right)\right] - \\ &- R[y\ln y + (1-y)\ln(1-y)]. \qquad (2.19) \end{aligned}$$

Summing over all trays yields the total entropy production

$$\Delta S^{\mathrm{u}} = \sum_{n=0}^{N} \Delta S_n^{\mathrm{u}} = \Delta S^{\mathrm{massflows}} - \sum_{n=0}^{N} \frac{Q_n}{T_n}, \qquad (2.20)$$

where $n = 0$ refers to the condenser and $\Delta S^{\mathrm{massflows}}$ is given by

$$\Delta S^{\mathrm{massflows}} = -F s_{\mathrm{F}}^{\mathrm{liq}} + D s_{\mathrm{D}}^{\mathrm{liq}} + B s_{\mathrm{B}}^{\mathrm{liq}}. \qquad (2.21)$$

$s_{\mathrm{F}}^{\mathrm{liq}}$, $s_{\mathrm{D}}^{\mathrm{liq}}$ and $s_{\mathrm{B}}^{\mathrm{liq}}$ denote the entropies per mole of feed, distillate and bottoms mass flow, respectively. Hence, the heat exchange between column and surroundings and the mass flows of distillate, bottoms and feed contribute to the entropy production ΔS^{u}. Since the column is in steady state, its entropy is constant. This implies that the entropy production equals the change in entropy of the column's surroundings.

Note that $\Delta S^{\mathrm{massflows}}$ is fixed by the specifications of the process and is therefore not part of the optimization.

2.2 Equal Thermodynamic Distance

In the following the asymptotic theory of equal thermodynamic distance (ETD) is briefly described. This theory provides a lower bound on the entropy production (2.20) of a fully diabatic distillation column, and will be later used to compare with the numerical analysis.

The concept of ETD uses a thermodynamic metric based on the entropy state function of the mixture to be separated. The thermodynamic length $\mathcal{L}$ of a process is given by the line element [22]

$$\mathrm{d}\mathcal{L} = \sqrt{-\mathrm{d}\mathbf{Z}^{\mathrm{t}}\, D^2 S\, \mathrm{d}\mathbf{Z}}. \tag{2.22}$$

where $\mathbf{Z} = (U, V, \ldots)$ is the vector of extensive variables and $D^2 S$ is the matrix of partial derivatives $\partial^2 S / \partial Z_i \partial Z_j$.

The distillation process is modeled as an N-step process [44], with N corresponding to the number of trays in the distillation column. There is an asymptotic theory bounding the entropy production for such processes in the limit of $N \to \infty$. Asymptotically, the total entropy production ΔS^{u} of an N-step process is bounded by

$$\Delta S^{\mathrm{u}} \geq \frac{\mathcal{L}^2}{2N} \tag{2.23}$$

This is a result from the horse-carrot theorem [22, 44]. The thermodynamic length of an N-step process can be written as

$$\mathcal{L} = \sum_{n=1}^{N} \Delta\mathcal{L}_n\,, \tag{2.24}$$

where $\Delta\mathcal{L}_n$ is the length of the n-th step. Asymptotically, for minimal entropy production the lengths of the steps have to be equal, i.e.

$$\Delta\mathcal{L}_1 = \ldots = \Delta\mathcal{L}_n = \ldots = \Delta\mathcal{L}_N\,, \tag{2.25}$$

hence the name, equal thermodynamic distance.

For the distillation model described in the previous section, the thermodynamic length element equation (2.22) is given by [22]

$$\mathrm{d}\mathcal{L} = \frac{\sqrt{C_\sigma}}{T}\,\mathrm{d}T\,, \tag{2.26}$$

where C_σ is the total constant pressure coexistence heat capacity of the binary two-phase mixture in equilibrium [45]. This is the heat capacity of a constant pressure system consisting of L moles of liquid coexisting in equilibrium with V moles of vapor. Its mathematical representation is given by

$$\begin{aligned} C_\sigma &= L\left[x\, c_{\mathrm{p}}^{\mathrm{liq},1} + (1-x)\, c_{\mathrm{p}}^{\mathrm{liq},2} + \frac{R\,T}{x\,(1-x)}\left(\frac{\mathrm{d}x}{\mathrm{d}T}\right)^2\right] \\ &+ V\left[y\, c_{\mathrm{p}}^{\mathrm{vap},1} + (1-y)\, c_{\mathrm{p}}^{\mathrm{vap},2} + \frac{R\,T}{y\,(1-y)}\left(\frac{\mathrm{d}y}{\mathrm{d}T}\right)^2\right]. \end{aligned} \tag{2.27}$$

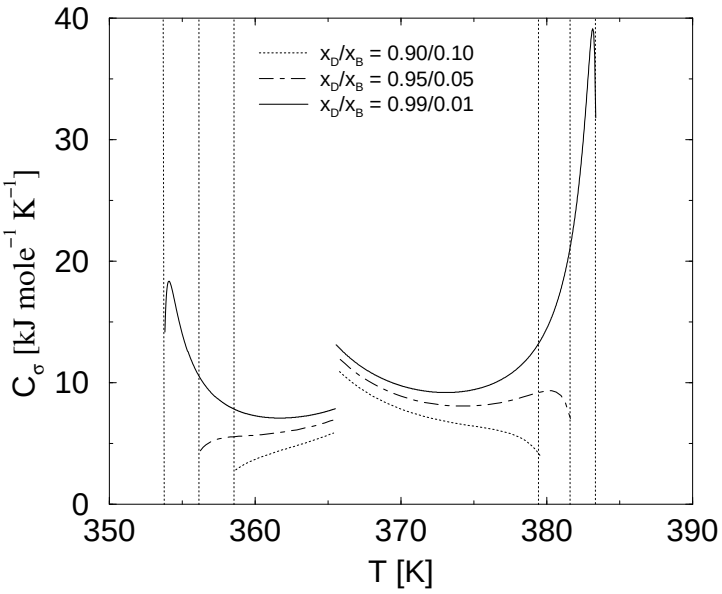

Figure 2.3: Heat capacity in equation (2.26) as a function of temperature for three different purity requirements. The vertical dotted lines show the corresponding highest and lowest temperatures in the column. The break at $T = 366\,\mathrm{K}$ shows the feed point.

As such a system is heated, the amounts of liquid and vapor change and the compositions readjust in such a fashion as to maintain equilibrium. The quantities of liquid and vapor that need to be counted in C_σ are the flows L and V between trays. To give $V(T)$ and $L(T)$ irrespective of N, these need to be taken equal to the limiting (infinite N) values which are given above the feed by

$$V(T) = \frac{x_\mathrm{D} - x(T)}{y(T) - x(T)} D, \tag{2.28}$$

$$L(T) = \frac{x_\mathrm{D} - y(T)}{y(T) - x(T)} D, \tag{2.29}$$

and below the feed by

$$V(T) = \frac{x(T) - x_\mathrm{B}}{x(T) - y(T)} B, \tag{2.30}$$

$$L(T) = \frac{y(T) - x_\mathrm{B}}{x(T) - y(T)} B. \tag{2.31}$$

In figure 2.3, C_σ of a benzene/toluene mixture is depicted for different purity requirements.

In order to establish an ETD path from the condenser T_0 to the reboiler T_N in a column with N trays, one has to determine temperatures T_n such that

$$\int_{T_n}^{T_{n+1}} \frac{\sqrt{C_\sigma}}{T}\,\mathrm{d}T \;=\; \frac{1}{N}\int_{T_0}^{T_N} \frac{\sqrt{C_\sigma}}{T}\,\mathrm{d}T\,, \qquad n = 0, \ldots, N-1\,. \tag{2.32}$$

The temperature profile obtained with the iteration above allows to calculate the entropy production (2.20) and all other relevant quantites. ETD is a first-order asymptotic theory [22, 27] for minimum entropy production in $1/N$. This gives rise to the question of how reliable ETD is for columns with few trays. In order to answer this question, a fully numerical, multidimensional optimization routine is applied to minimize the entropy production in a diabatic distillation column and to further compare the results with ETD.

Chapter 3

Numerical Optimization

Previous studies of diabatic distillation columns using the ETD approach have shown enormous exergy savings compared to conventional distillation for columns with a large number of trays (e. g. [21]). But because of the asymptotic nature of ETD, the true minimum will be lower for fewer trays. Consequently, one is interested in the difference between ETD and optimal operation. This motivates a fully numerical optimization which will find the true minimum for any feasible number of trays.

The entropy production (2.20) is minimized using a multidimensional optimization routine. The tray temperatures T_n, $n = 1, \ldots, N$ are used as the control variables, thus the optimal temperature of each tray in the column is determined without applying any thermodynamic principle like ETD. Once knowing the optimal temperature profile, one can easily compute all the corresponding quantities like heat demand per tray, liquid and vapor flows entering/leaving each tray and molar fractions of the liquid and vapor phase.

Calculating the gradient of equation (2.20) is rather costly due to the structure of the state equations (2.5) and (2.6). For this reason, Powell's method [46] is chosen to perform the minimizations since it does not require gradient information. A more detailed description of Powell's algorithm is given in Appendix A.

This chapter gives a detailed comparison of ETD columns, numerically optimized and conventional columns. Besides looking at the total entropy production of each column type, the resulting operation profiles of the columns (e. g. heat requirement per tray) are studied as well. The optimal profiles allow to give design recommendations for diabatic columns. Results presented in this chapter are also published in [35, 42].

3.1 Problem Definition

Appropriate penalty functions have to be added to the entropy production in order to take into account the physical constraints on the optimization problem. In this section it is also shown how the entropy production of a conventional column can be expressed as an optimization problem.

3.1.1 Diabatic Column

The entropy production (2.20) consists of terms of the form Q_n/T_n which in turn are functions of the liquid and vapor flows V_n and L_n. An explicit representation of the vapor flow above the feed using the material balance (2.3) and (2.4) is given by

$$V_n(T_n, T_{n-1}) = \frac{x_\mathrm{D} - x_{n-1}(T_{n-1})}{y_n(T_n) - x_{n-1}(T_{n-1})} D. \tag{3.1}$$

Analogous expressions exist for the liquid flows and the trays below the feed. Equation (3.1) has a singularity, the flow becomes infinite for $y_n = x_{n-1}$. This implies the physical constraint

$$x_{n-1} < y_n, \tag{3.2}$$

i. e., the molar fraction in the vapor coming up from tray n has to be larger than the molar fraction in the liquid going down from tray $n-1$. This in turn means that the difference between the temperatures of two adjacent trays must be restricted so that the constraint above is fulfilled. Violating this constraint leads to unphysical results, e. g. negative values of liquid and vapor flows.

The temperature T_1 at the uppermost tray as well as the temperature T_N at the reboiler are fixed by the given distillate and bottoms purity requirements x_D and x_B respectively. This reduces the number of control variables to $N-2$. Defining the control vector $\mathbf{T} = (T_2, \ldots, T_{N-1})$, the minimization problem then takes the form

$$\Delta S^{\mathrm{u,opt}} = \min_{\mathbf{T}} \left(-\sum_{n=0}^{N} \frac{Q_n}{T_n} + \mathcal{P}(\mathbf{T}) \right) + \Delta S^{\mathrm{massflows}}. \tag{3.3}$$

Again, here $n = 0$ refers to the condenser. $\mathcal{P}(\mathbf{T})$ denotes a penalty function which is added to the entropy production when constraint (3.2) is not fulfilled.

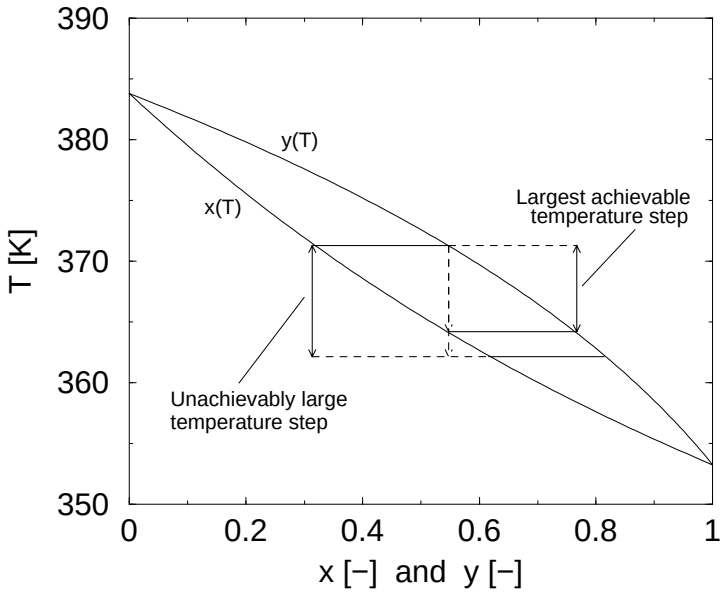

Figure 3.1: Description of an unphysical situation in the liquid-vapor-diagram. When the temperature difference between two adjacent trays is too large, constraint (3.2) is not fulfilled.

The penalty is written as

$$\mathcal{P}(\mathbf{T}) = M \sum_{n=1}^{N-1} \Theta(x_n - y_{n+1})(x_n - y_{n+1})^2, \tag{3.4}$$

where $\Theta(.)$ denotes the Heaviside function and M is a sufficiently large number. Powell's method is then applied to equation (3.3) to obtain minimum entropy production and the corresponding optimal temperature profile.

3.1.2 Conventional Column

A calculation method to determine the temperature profile of a conventional column is required in order to compare the performance of a diabatic column with its adiabatic counterpart. A common way to obtain the temperature profile are shooting methods. But here a novel approach is given by formulating the entropy production of a conventional column as a minimization problem. One still uses the model for diabatic distillation given in section 2.1, but takes the reflux L_0 to be a positive quantity, as required for the conventional column.

In a conventional column, the amount of condenser heat Q_{D} can be controlled by the reflux L_0 (see equation (2.12)). For this reason L_0 is added to the control vector $\mathbf{T}$ and a second term is added to the penalty function (3.4). This term prevents the reflux from becoming negative during the optimization. Hence, the new penalty takes the form

$$\mathcal{P}(\mathbf{T}) = M_1[1 - \Theta(L_0)]L_0^2 + M_2 \sum_{n=1}^{N-1} \Theta(x_n - y_{n+1})(x_n - y_{n+1})^2, \tag{3.5}$$

where M_1 and M_2 denote sufficiently large numbers. We introduce another penalty function of the form

$$\mathcal{Q}(\mathbf{T}) = M_3 \sum_{n=1}^{N-1} Q_n^2, \tag{3.6}$$

where M_3 is some constant turning the squared heats into the dimension of an entropy. The latter penalty causes the intermediate heat requirements of the diabatic column to be 'turned off' during the optimization. The penalties vanishing, only the entropy flows of condenser and reboiler account for the entropy production which we then can express as

$$\Delta S^{\mathrm{u,conv}} = \min_{\mathbf{T}} \left(\mathcal{P}(\mathbf{T}) + \mathcal{Q}(\mathbf{T}) - \frac{Q_{\mathrm{D}}}{T_{\mathrm{D}}} - \frac{Q_{\mathrm{B}}}{T_{\mathrm{B}}} \right) + \Delta S^{\mathrm{massflows}}. \tag{3.7}$$

Thus, it is now possible to use Powell's method for both diabatic and conventional column.

3.2 Optimization Results

A benzene/toluene mixture is chosen as our system to be separated. The most important thermal properties are listed in Table 3.1. The entropy production for the separation of a 50/50 mole fraction benzene/toluene mixture is minimized by applying ETD and numerical optimization and compared to the corresponding conventional column. The number of trays and purity requirements are varied to show differences in the performance of ETD and numerical minimizations. The comparisons are always between columns with the same material flows in and out. Notably the feed, bottoms and distillate flows match not only in magnitude but also in composition and temperature in the columns compared.

Table 3.1: Important thermal properties of pure benzene and toluene

Property	Benzene	Toluene
Boiling temperatures [K]	353.25	383.78
Heat capacity, vapor phase [$\mathrm{J\,mole^{-1}K^{-1}}$]	81.63	106.01
Heat capacity, liquid phase [$\mathrm{J\,mole^{-1}K^{-1}}$]	133.50	156.95
Heat of evaporization [$\mathrm{J\,mole^{-1}}$]	33600	38000
Reference entropies at 298 K [$\mathrm{J\,mole^{-1}K^{-1}}$]	269.20	319.74

3.2.1 Numerical Performance

Powell's minimization routine only allows to find local minima. Therefore various runs with a wide range of different initial guesses are necessary for calculating the minimum entropy production of a distillation column. Thus, one can test whether different starting values lead to different local minima. Random starting vectors are produced the following way: the temperature in both conventional and diabatic columns is bounded by the fixed values T_1 and T_N, so $N-2$ random temperatures within the range $[T_1 \dots T_N]$ are determined. Subsequent sorting of these temperatures then yield a random initial temperature vector for the optimization procedure.

Initial guesses as described above are applied to the objective functions (3.3) and (3.7). Multiple minimization runs for a given number of trays do not reveal different local minima. Hence, the resulting minimum value for the entropy production is most probably the global minimum. All what could be observed was a slight dependence of the number of Powell iterations on the initial guess. A good guess, i.e. close to the optimum control vector, reduced the amount of computations.

Throughout all minimizations, a relative accuracy of 10^{-9} was used. For shorter columns ($N < 30$) it takes less than $10N$ Powell itertions to get to the minimum. But the computational effort increases considerably once longer columns ($N > 50$) are optimized. In these cases it needed up to several $100N$ Powell iterations until the minimum was found.

Surprisingly, the evaluation of the entropy production for the conventional column (equation (3.7)) is much more costly than the optimization of the diabatic counterpart. Even for short columns it takes several $100N$ Powell iterations until the minimum. For longer columns the effect is even more

dramatic, requiring more than $10^5 N$ Powell iterations. Apparently, the slow convergence is due to the $\sum_n Q_n^2$ term in equation (3.7).

3.2.2 Total Entropy Production

First, we look at the entropy production as a function of the number of trays for all three types of distillation columns. The results for the simulations are shown in figures 3.2–3.4 for three different purity requirements. The figures include curves for

- a conventional column calculated with equation (3.7)
- the corresponding ETD column determined by equation (2.32)
- the numerically optimized column (equation (3.3))
- and the aymptotic lower bound $\mathcal{L}^2/(2N)$ for the entropy production based on the ETD calculation.

For all three purity requirements the optimal diabatic columns are far more efficient than their conventional adiabatic counterparts. In the small N region, the entropy production is reduced by about 15–30%, for columns with many trays one can find reductions of 65–80%. For short columns, the numerical optimization results predict slightly less entropy production; the optimal values are up to 10% lower than the corresponding ETD values. For larger N values ETD agreed very well with the numerical minimization. The optimal results also were above the ETD lower bound $\mathcal{L}^2/(2N)$, but approached the ETD bound as N was increased. The large N simulation for the 99/01 purity requirement had the closest values to the ETD bound as was expected due to the asymptotic nature of the ETD theory.

For a certain total thermodynamic length $\mathcal{L}$ and number of trays N, each ETD step must go a distance $\mathcal{L}/N$. When N is below a certain value, condition (3.2) does not hold anymore because the thermodynamic distance (and hence the temperature difference) between two adjacent trays is too large. Since this leads to unphysical results ETD and its lower bound is not plotted for $N < 13$ for the 95/05 separation and $N < 32$ for the 99/01 separation. This is a serious limitation of the ETD theory and makes it only applicable for sufficiently long columns.

The $\mathcal{L}^2/2N$ values are suprisingly far from the ETD curves. The reason for this comes from the fact that the flow rates V and L enter the expression

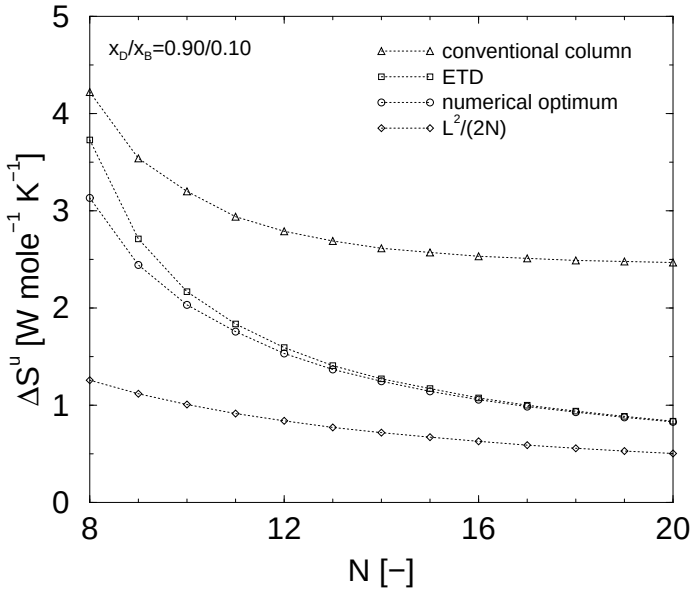

Figure 3.2: Minimal entropy production for varying number of trays determined with ETD and numerical optimization. The required purity is $x_{\mathrm{D}} = 0.90$, $x_{\mathrm{B}} = 0.10$. For comparison, the entropy production for a conventional column and the lower bound for ETD, $\mathcal{L}^2/(2N)$ is included.

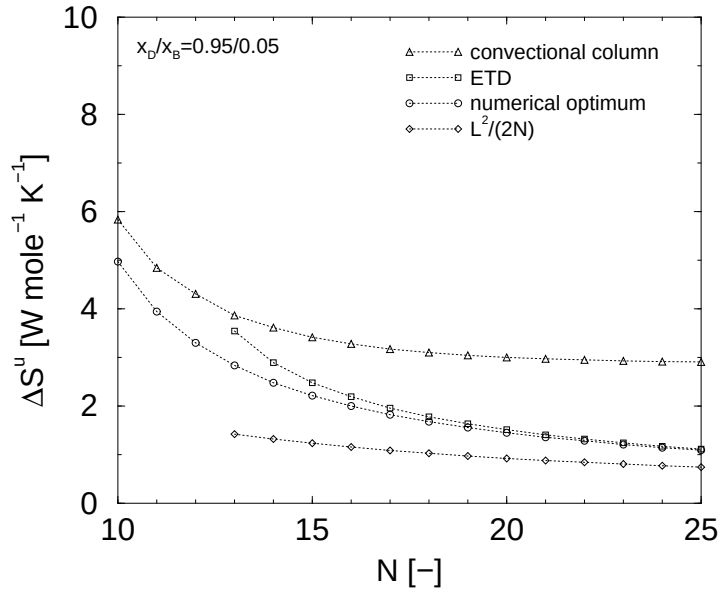

Figure 3.3: Minimal entropy production for $x_{\mathrm{D}} = 0.95$, $x_{\mathrm{B}} = 0.05$.

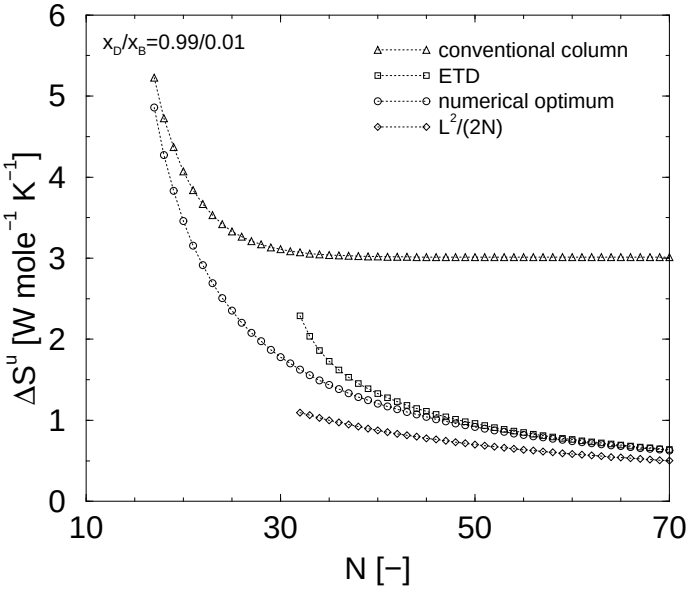

Figure 3.4: Minimal entropy production for $x_{\mathrm{D}} = 0.99$, $x_{\mathrm{B}} = 0.01$.

for C_σ. The values of V and L are the continuous values given in equation (2.26) which corresponds to an infinite number of trays. The continuous path is needed to define thermodynamic distance along the column. When the temperatures found from equation (2.32) are used to calculate the actual flow rates with the given number of trays N, the flow rates are significantly above the minimum reflux levels and account for the difference[1]. The surprisingly good match between $\Delta S^{\mathrm{u,opt}}$ and $\Delta S^{\mathrm{u,ETD}}$ leads to a deeper explanation [47]. There, it turns out that the difference between these two quantities is always of order $1/N^3$.

3.2.3 Operating Profiles

Next we investigate the operating profiles of three columns with different number of trays and purity requirements. Temperature profiles, heat requirements per tray, and the distribution of entropy production along the column, as well as the liquid and vapor flows, and the molar fractions of liquid and vapor phase, are shown for a 15 tray columns with a 90/10 separation (figure 3.5 and 3.6), a 25 tray columns with a 95/05 separation (figure

[1]This reflux rate refers to the value of $V - L$ for that tray and should not be confused with the reflux rate L_0 for the column which is needed to be non-zero for the conventional column but is zero for the ETD and the optimal columns.

3.7 and 3.8), and a 70 tray column with a 99/01 separation (figure 3.9 and 3.10). In each figure, the profiles are plotted for an optimized column, an ETD column and the corresponding conventional column.

Tray Temperatures

The temperature profiles for both ETD and optimal show a characteristic mild 'S' curvature found in optimally operating column where the separation is symmetric. This shape of the temperature profiles is probably due to the effective heat capacity C_σ. The temperature difference from tray to tray in the column is smaller in the regions where the heat capacity is large. As can be seen in figure 2.3, the 99/01 separation is the most dramatic example. By contrast, the temperature profile of the conventional column is much steeper in the top and bottom part but has a plateau in the middle of the column around the feed point. For longer columns and higher purity requirement this shape becomes more distinct, as can be seen from the temperature profile of the 70 tray column (figure 3.9).

Material Flows and Concentration Profiles

The liquid and vapor flows are roughly constant over the column length in the conventional column, apart from the jump of the liquid flow curve on the feed tray. In the diabatic case, the flow rates decrease from the feed point towards the top and bottom part of the column. As the flow rates are significantly smaller than in the conventional column, some of the column's cross sectional area can be alloted for the heat exchangers to be installed without interfering with the material flows.

The molar fractions follow the shape of the temperatur profiles, indicating a more evenly distributed separation inside the diabatic column, as opposed to the plateau in the middle of the conventional one, where no separation takes place.

Entropy Production per Tray

The temperature profiles also reflect the distribution of the entropy production along the column. While the entropy production per tray is roughly the same for all trays in the diabatic case, there are two huge peaks in the top and bottom part of the conventional column, where all the energy degradation takes place. This situation becomes more dramatic with increasing

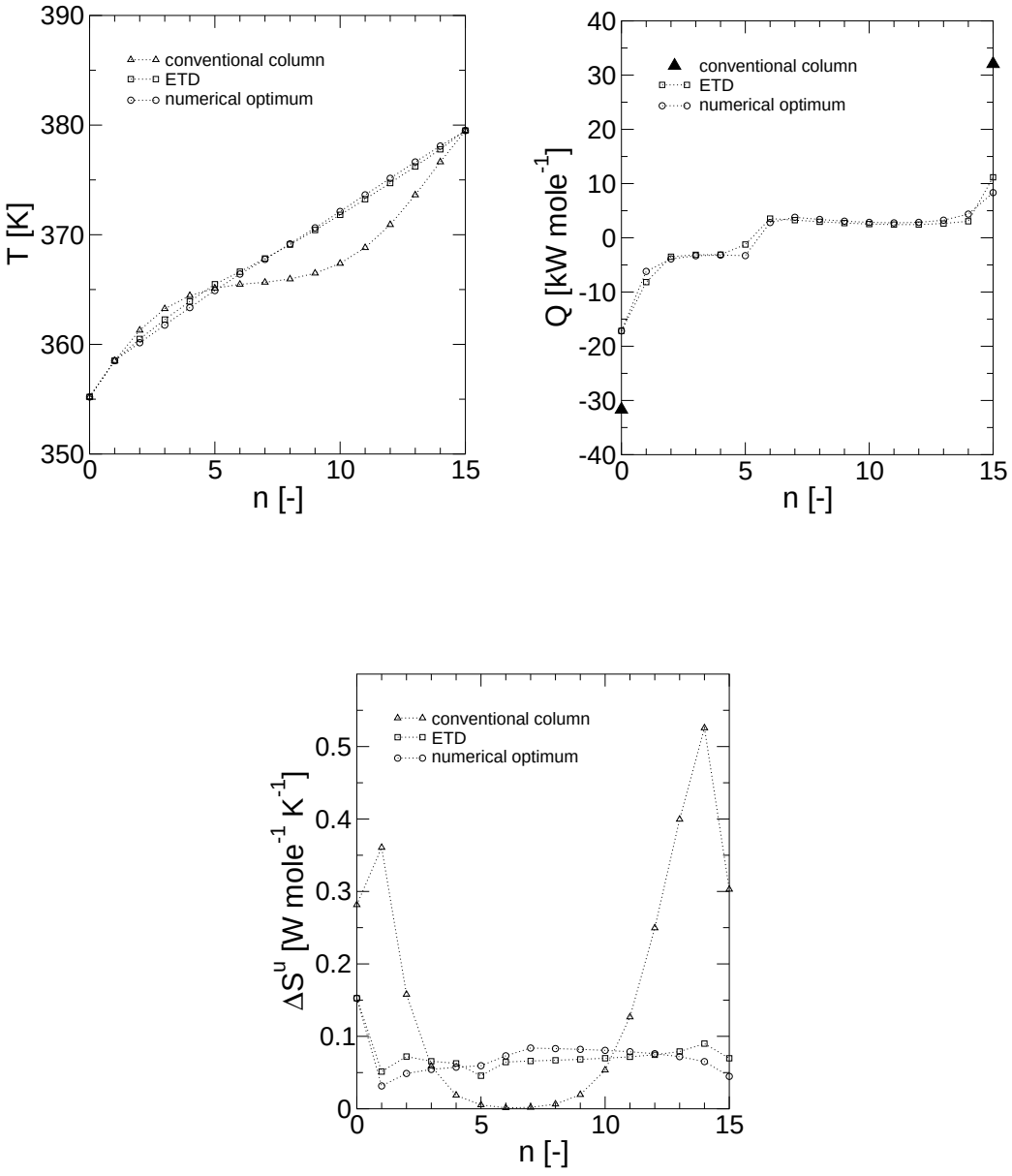

Figure 3.5: Temperature profile T, heating requirement Q, and entropy production ΔS^{u} per tray for a conventional column, an ETD column and a numerically optimized column with 15 trays. The required purity is $x_{\mathrm{D}} = 0.90$, $x_{\mathrm{B}} = 0.10$.

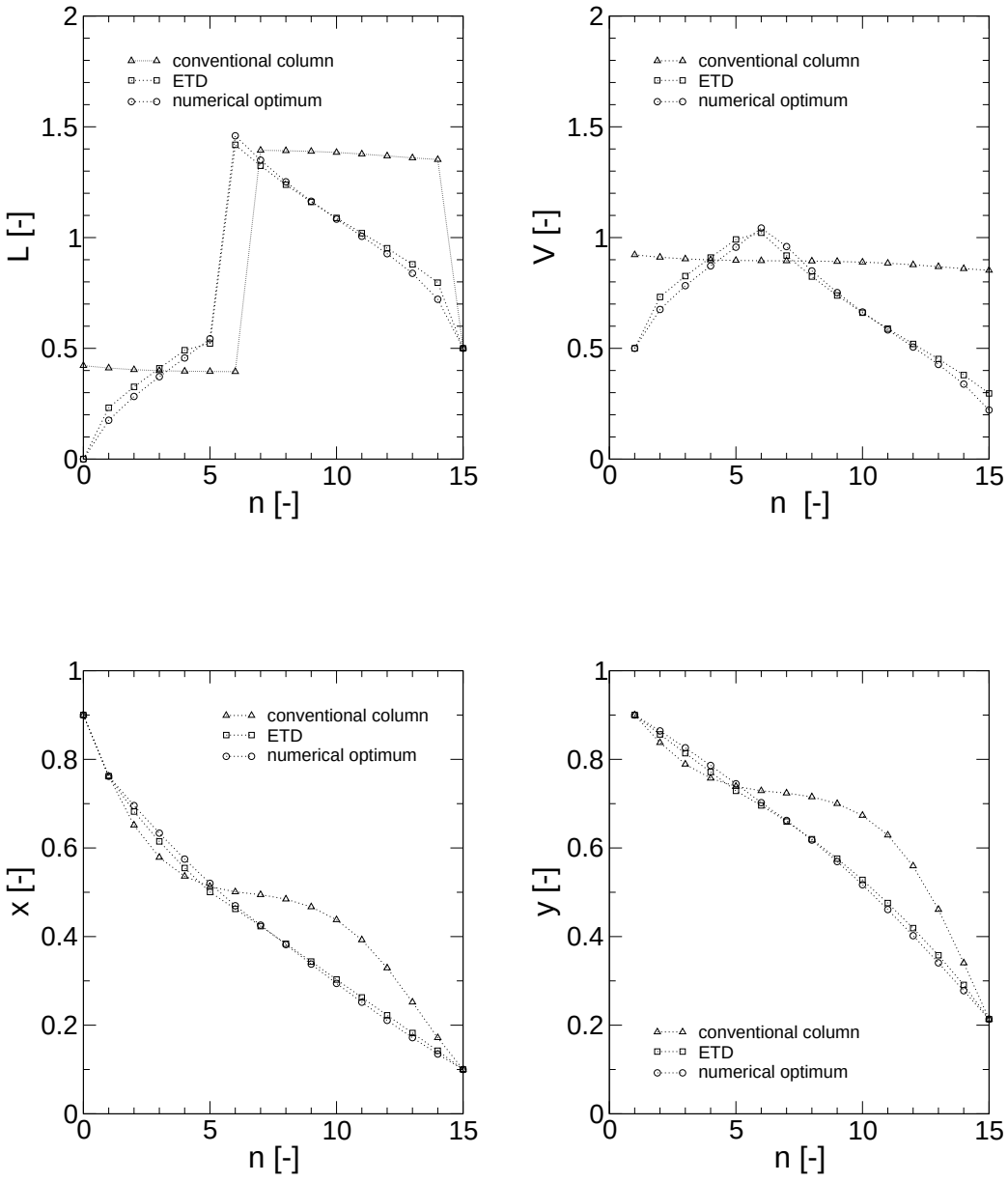

Figure 3.6: Liquid flow L, vapor flow V, molar fraction x of liquid phase, and molar fraction y of vapor phase, for a conventional column, an ETD column and a numerically optimized column with 15 trays. The required purity is $x_{\mathrm{D}} = 0.90$, $x_{\mathrm{B}} = 0.10$.

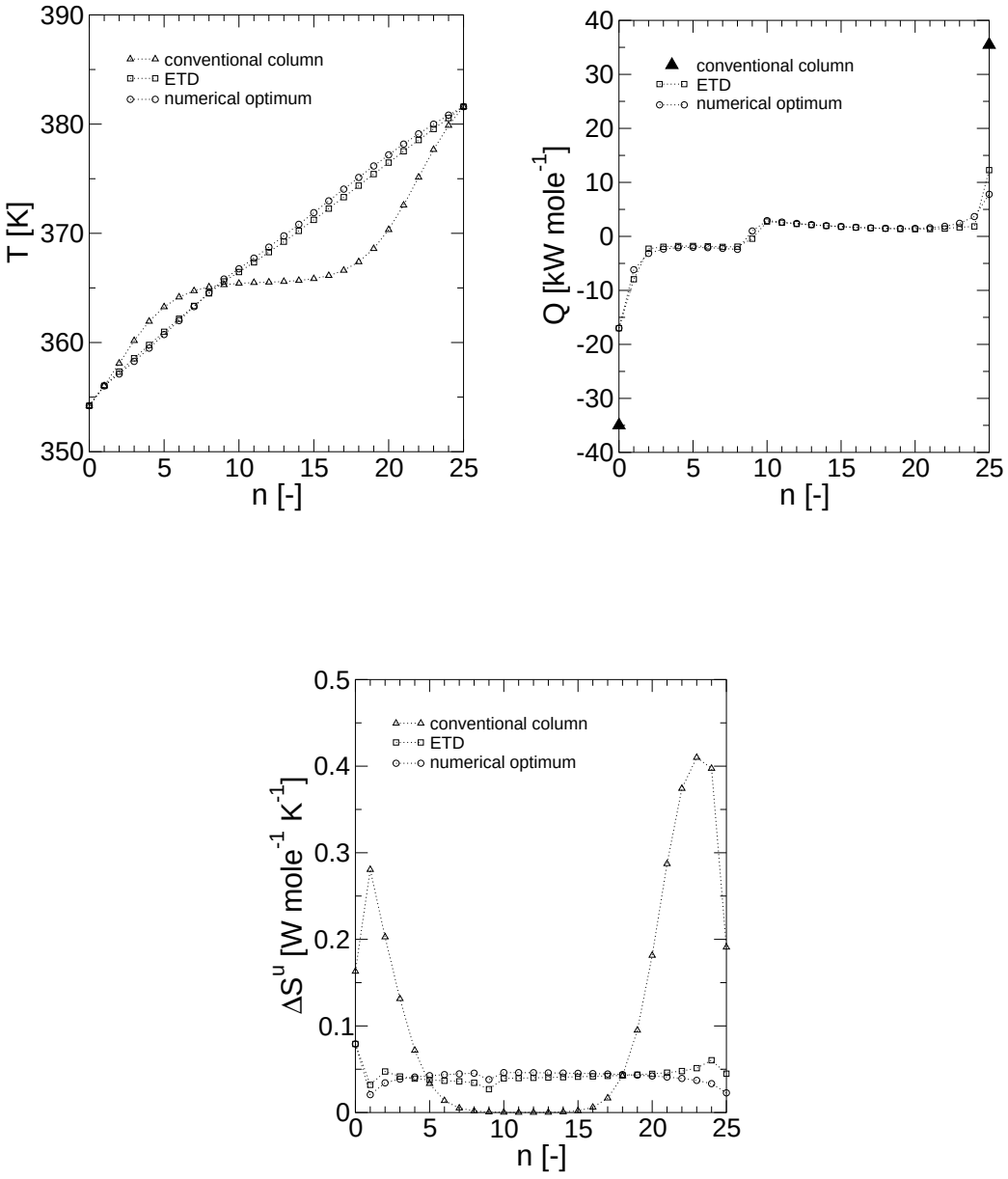

Figure 3.7: Temperature profile T, heating requirement Q, and entropy production ΔS^{u} per tray for a conventional column, an ETD column and a numerically optimized column with 25 trays. The required purity is $x_{\mathrm{D}} = 0.95$, $x_{\mathrm{B}} = 0.05$.

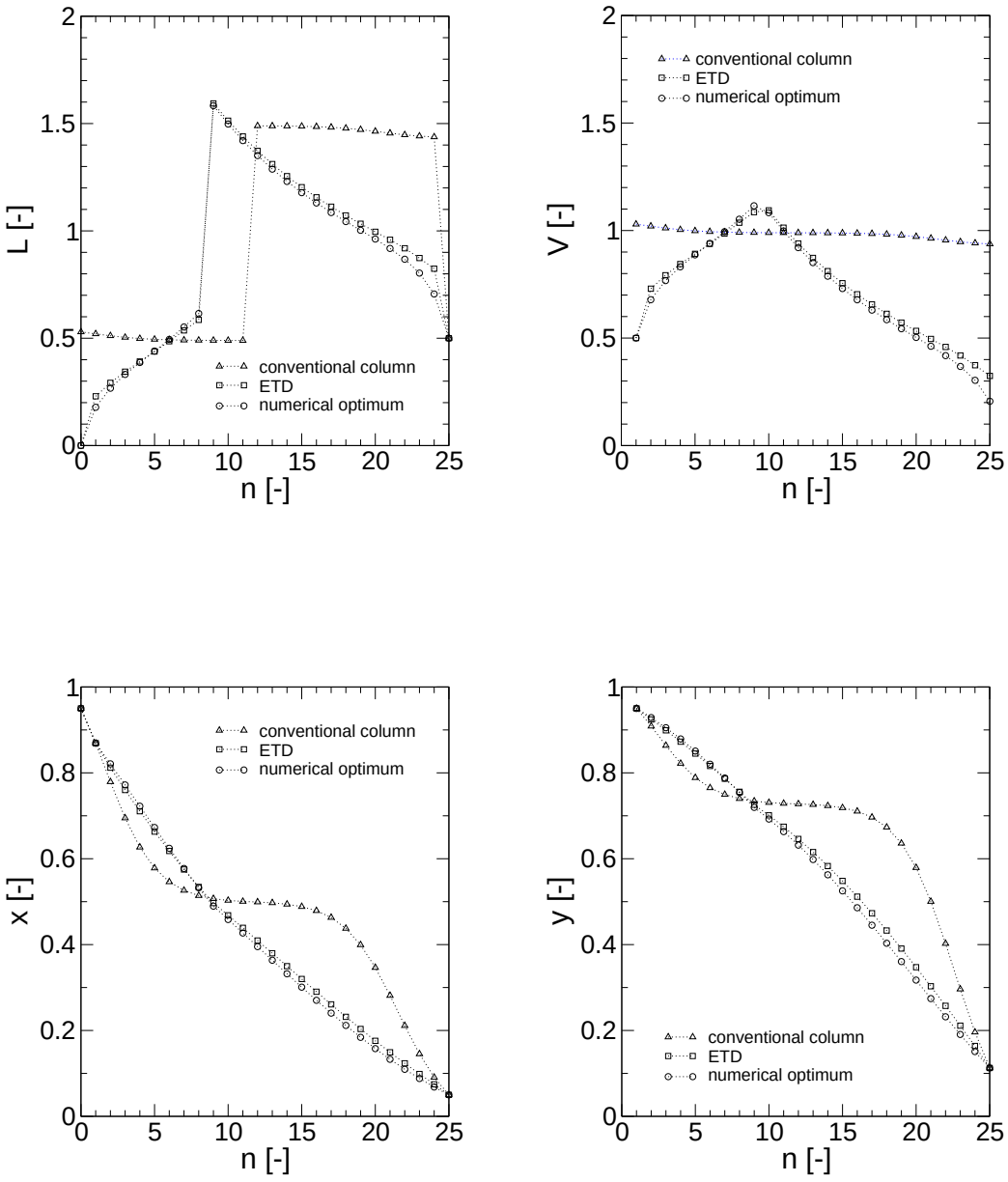

Figure 3.8: Liquid flow L, vapor flow V, molar fraction x of liquid phase, and molar fraction y of vapor phase, for a conventional column, an ETD column and a numerically optimized column with 25 trays. The required purity is $x_{\mathrm{D}} = 0.95$, $x_{\mathrm{B}} = 0.05$.

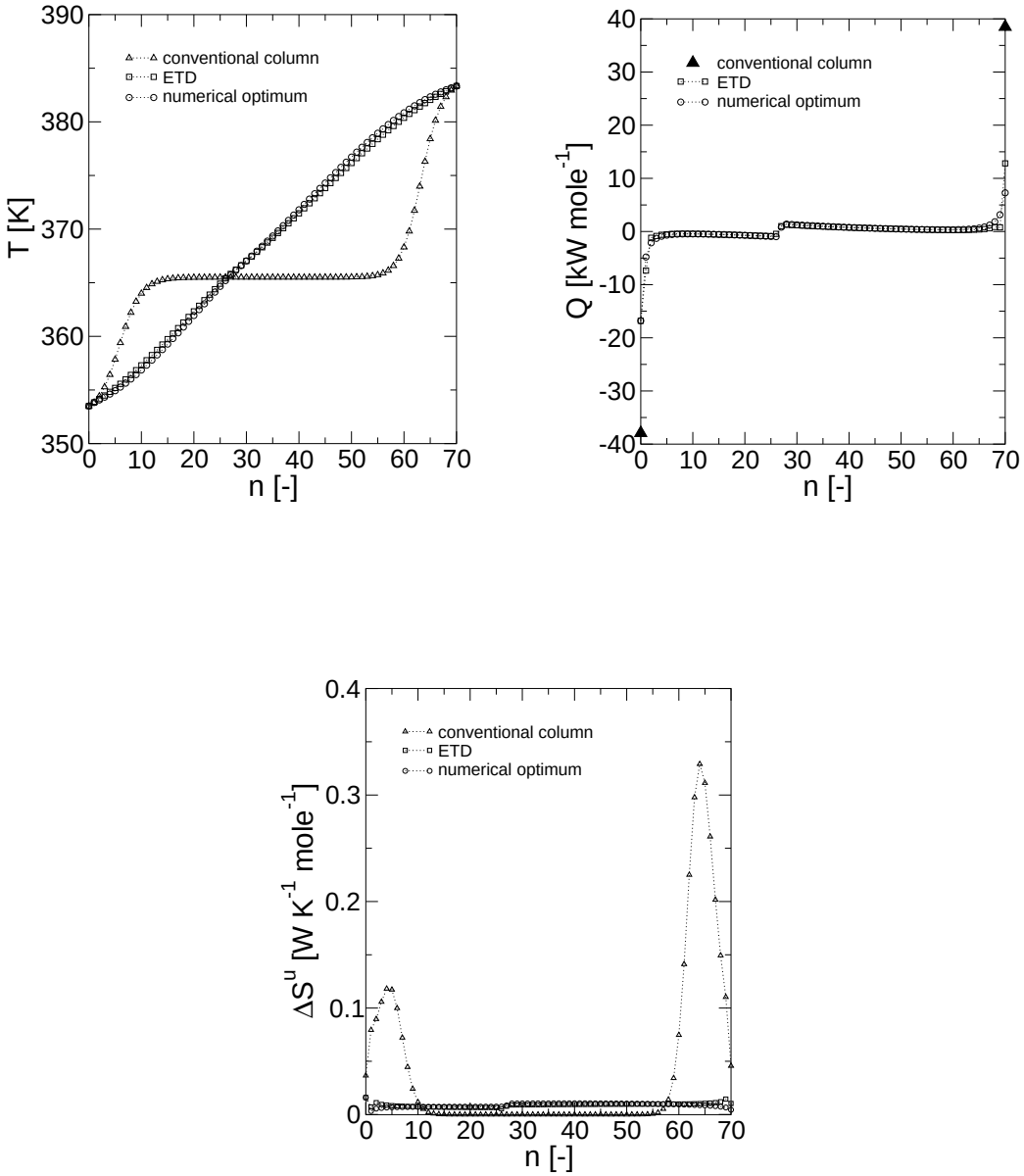

Figure 3.9: Temperature profile T, heating requirement Q, and entropy production ΔS^{u} per tray for a conventional column, an ETD column and a numerically optimized column with 70 trays. The required purity is $x_{\mathrm{D}} = 0.99$, $x_{\mathrm{B}} = 0.01$.

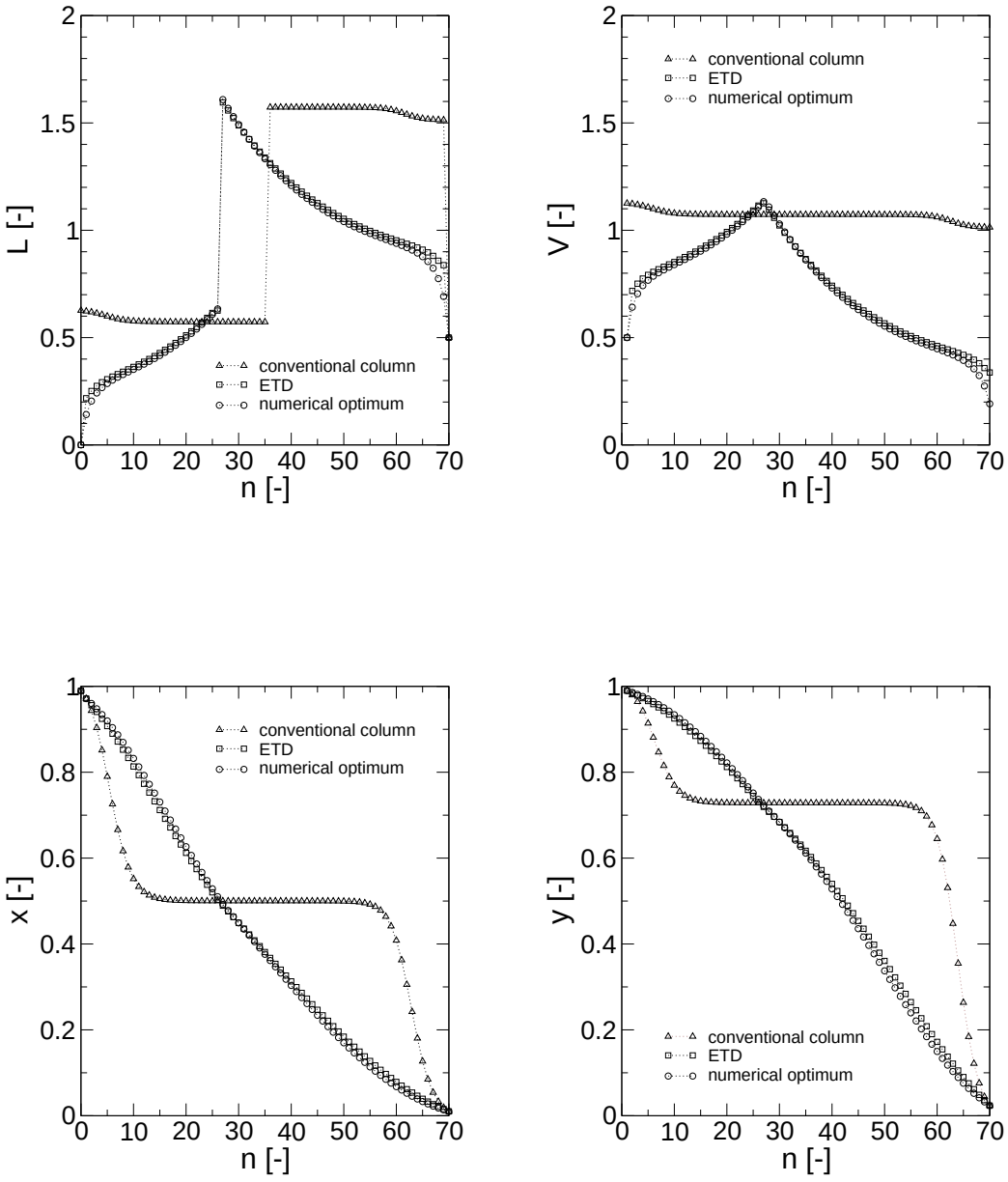

Figure 3.10: Liquid flow L, vapor flow V, molar fraction x of liquid phase, and molar fraction y of vapor phase, for a conventional column, an ETD column and a numerically optimized column with 70 trays. The required purity is $x_{\mathrm{D}} = 0.99$, $x_{\mathrm{B}} = 0.01$.

column length. In the region of the temperature plateau there is no entropy production. It is also remarkable that the numerically optimized diabatic column produces more entropy in the middle section than the ETD column. But in the top and bottom part the optimal column is more efficient than the ETD column. In the optimal column the thermodynamic distance between two adjacent trays is less than the ETD step ($\mathcal{L}/N$) near the condenser and the reboiler, whereas in the middle section it is larger than $\mathcal{L}/N$.

Heating and Cooling Duties

This is also the reason for the differences between the optimal and the ETD heating profiles. The figures show that in general the ETD column requires larger condensers and reboilers than the optimal column but smaller heat exchangers on intermediate trays. Since squeezing large heat exchangers into distillation trays has proved to be a difficult task, this may be a desirable feature for some installations. Another thing to note is that the heat demands for the intermediate trays are fairly small and roughly the same for all the trays. On closer examination of the heat demand for the 70 tray column, we note that the demands near the feed and near the reboiler and condenser are significantly higher than the demands on the trays in between. This gives the familiar (inverted-u)-u shape shown in figure 3.11 previously noted in other studies [21, 27, 35, 36]. A similar examination of the 15 tray column shows only a slight tendency toward this behavior and keeps $|Q_n| \approx$ constant for $1 < n < N$. Nearly constant heat demand makes Rivero's design for diabatic columns quite attractive [30]. His design employs two heat exchanger circuits: one above and one below feed. Each heat exchanger winds its way through the column and this arrangement can probably approximate the optimal heating/cooling profiles found here.

3.3 Summary

The entropy production associated with diabatic distillation is minimized using Powell's method. This allows a detailed comparison with results obatined from the asymptotic ETD theory and conventional adiabatic distillation columns. The entropy production of the latter is also formulated as a minimization problem. An optimal diabatic column offers enormous reduction of entropy production compared to its adiabatic counterpart. Some striking values are listed in table 3.2. For columns with fewer trays, numerical

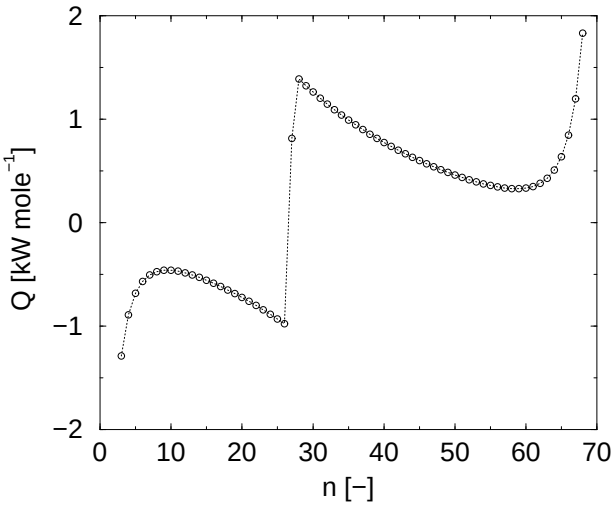

Figure 3.11: The familiar (inverted-u)-u shape of the optimal heating profile. Data shown are the same as in the heat duty profile of figure 3.9 with end trays omitted.

optimization yields slightly better results than ETD. In this case there are significant deviations, particularly in the heating profiles. For longer columns, the optimal profile calls for a nearly constant heat demand, which works well with the Rivero implementation of diabatic columns [30, 32].

Table 3.2: Comparison of entropy production for conventional and optimized diabatic distillation columns.

column	x_D/x_B	$\Delta S^{\mathrm{u}}_{\mathrm{conv}}$	$\Delta S^{\mathrm{u}}_{\mathrm{opt}}$	savings
15 trays	0.90/0.10	2.57	1.14	56%
25 trays	0.95/0.05	2.90	1.09	62%
70 trays	0.99/0.01	3.01	0.62	79%

Chapter 4

Heat Transfer Irreversibilities

The numerical study presented in Chapter 3 has focused on the entropy production *inside* the column while relegating to the environment the entropy production associated with getting the requisite heat exchanges to happen at desired rates.

This chapter considers the question of how this heat exchange, when included in the entropy production minimization, affects the optimal heating profile for fully diabatic columns. In the absence of counting irreversibilities due to heat exchange between the column and its surroundings, the optimal profile is independent of rate of operation in the sense that the optimal profile scales directly with the feed rate. Usually the purities of the feed, distillate and bottoms are specified so that a given feed rate F determines the rate of distillate and bottoms production through

$$D = \frac{x_{\mathrm{F}} - x_{\mathrm{B}}}{x_{\mathrm{D}} - x_{\mathrm{B}}} F \stackrel{\mathrm{def}}{=} d\,F \tag{4.1}$$

$$B = \frac{x_{\mathrm{F}} - x_{\mathrm{D}}}{x_{\mathrm{B}} - x_{\mathrm{D}}} F \stackrel{\mathrm{def}}{=} b\,F. \tag{4.2}$$

Letting

$$q_n = Q_n/F \tag{4.3}$$

one can rewrite the entropy production (2.20) using the definitions of d and b from equations (4.1) and (4.2)

$$\Delta S^{\mathrm{u,sep}} = F\left(-s_{\mathrm{F}}^{\mathrm{liq}} + d s_{\mathrm{D}}^{\mathrm{liq}} + b s_{\mathrm{B}}^{\mathrm{liq}} - \sum_{n=0}^{N} \frac{q_n}{T_n}\right). \tag{4.4}$$

All the flows in the column are proportional to the feed rate F. This makes it natural that current studies [21, 25, 35, 42] all optimize the entropy production per feed rate. But the scaling behavior above is no longer the case

once the irreversibilities of the heat coupling to the outside of the column are included.

To explore the effects of non-vanishing heat exchange which must in fact proceed across a finite temperature difference and therefore produce entropy, we introduce two simple models for the heat transfer into the trays, the Newton and Fourier laws.

4.1 Entropy Production due to Heat Exchange

The entropy production due to the heat exchange to the n-th tray is

$$\Delta S_n^{\mathrm{u,hx}} = Q_n \left(\frac{1}{T_n} - \frac{1}{T_n^{\mathrm{ex}}} \right). \tag{4.5}$$

For a given amount of heat transferred Q_n, the required external temperature T_n^{ex} depends on our assumed heat transfer law. This law relates the heat transferred to the tray to the temperature T_n inside the tray and to the temperature T^{ex} in the heat exchange fluid outside the column. With our choice of the internal temperature profile as the control parameter, it is convenient to eliminate this dependence on the external temperatures by solving for the external temperature in terms of the heat transferred and the internal temperature and to use the resulting expression to eliminate T_n^{ex} in equation (4.5). This is carried out below for both of our heat transfer laws.

Note that with this procedure the entire optimization, including the losses in the heat exchangers, is still parametrized solely by the internal temperature. The external temperatures do not add a new degree of freedom but are consequences of the internal profile.

4.1.1 Fourier Heat Conduction

The first model is Fourier's law of heat transfer. Here the transfer is taken to be proportional to the difference of the inverse temperatures, i. e. to the thermodynamic force,

$$Q_n = \kappa_{\mathrm{FL}} \left(\frac{1}{T_n} - \frac{1}{T_n^{\mathrm{ex}}} \right), \quad \kappa_{\mathrm{FL}} > 0. \tag{4.6}$$

where κ_{FL} is the conductance of the contact between tray n at temperature T_n and a bath at temperature T_n^{ex}.

Solving for $1/T_n^{\mathrm{ex}}$ in equation (4.6) one finds

$$\frac{1}{T_n^{\mathrm{ex}}} = \frac{1}{T_n} - \frac{Q_n}{\kappa_{\mathrm{FL}}}, \tag{4.7}$$

which is substituted into equation (4.5) to yield the very simply expression, independent of temperatures,

$$\Delta S_n^{\mathrm{u,hx}} = \frac{Q_n^2}{\kappa_{\mathrm{FL}}}. \tag{4.8}$$

To make the feed rate dependence explicit, the quantity

$$g_{\mathrm{FL}} = \frac{F}{\kappa_{\mathrm{FL}}}, \tag{4.9}$$

is introduced, which describes the relative rate of mass and heat flow. One then can express equation (4.8) with $q = Q/F$ as

$$\Delta S_n^{\mathrm{u,hx}} = F g_{\mathrm{FL}} q_n^2. \tag{4.10}$$

Summing this over N trays, the total entropy production can be written as

$$\Delta S^{\mathrm{u}} = \Delta S^{\mathrm{u,sep}} + \Delta S^{\mathrm{u,hx}} \tag{4.11}$$

$$= F\left(-s_{\mathrm{F}}^{\mathrm{liq}} + d s_{\mathrm{D}}^{\mathrm{liq}} + b s_{\mathrm{B}}^{\mathrm{liq}} - \sum_{n=0}^{N} \frac{q_n}{T_n} + g_{\mathrm{FL}} \sum_{n=0}^{N} q_n^2\right). \tag{4.12}$$

Here it is evident that only the internal temperatures T_n are needed to parametrize the full operation of the column. They appear only in the entropy production term due to the internal separation, not in the term from the heat exchangers.

4.1.2 Newtonian Heat Conduction

In the second more conventional model, Newtonian heat conduction, the heat transfer is taken to be proportional to the difference of the temperatures,

$$Q_n = \kappa_{\mathrm{NL}}\left(T_n^{\mathrm{ex}} - T_n\right), \quad \kappa_{\mathrm{NL}} > 0, \tag{4.13}$$

Proceeding in the same fashion as in the previous subsection by eliminating T_n^{ex} in equation (4.5) one finds

$$\frac{1}{T_n^{\mathrm{ex}}} = \frac{1}{T_n + \dfrac{Q_n}{\kappa_{\mathrm{NL}}}}, \tag{4.14}$$

and thus

$$\Delta S_n^{\mathrm{u,hx}} = \frac{F^2}{\kappa_{\mathrm{NL}}} \frac{q_n^2}{T_n \left(T_n + \dfrac{F}{\kappa_{\mathrm{NL}}} q_n \right)} \tag{4.15}$$

$$= F g_{\mathrm{NL}} \frac{q_n^2}{T_n (T_n + g_{\mathrm{NL}} q_n)}, \tag{4.16}$$

with $g_{\mathrm{NL}} = F/\kappa_{\mathrm{NL}}$.

This results in a total entropy production of

$$\Delta S^{\mathrm{u}} = \Delta S^{\mathrm{u,sep}} + \Delta S^{\mathrm{u,hx}} \tag{4.17}$$

$$= F \left(-s_{\mathrm{F}}^{\mathrm{liq}} + d s_{\mathrm{D}}^{\mathrm{liq}} + b s_{\mathrm{B}}^{\mathrm{liq}} - \sum_{n=0}^{N} \frac{q_n}{T_n} + g_{\mathrm{NL}} \sum_{n=0}^{N} \frac{q_n^2}{T_n (T_n + g_{\mathrm{NL}} q_n)} \right). \tag{4.18}$$

Note that for $q_n < 0$ (heat being withdrawn from the column), the value of g_{NL} is limited to be in the range between 0 and $\min_n(T_n/q_n)$. The limit $g_{\mathrm{NL}} = 0$ corresponds to vanishing feed rate or infinitely fast heat exchange while the limit $g_{\mathrm{NL}} = \min_n(T_n/q_n)$ corresponds to the highest possible rate of heat removal for which $T_n^{\mathrm{ex}} = 0$.

4.2 Numerical Results

As model systems, three columns of different length (25, 45 and 65 trays) are chosen to separate an ideal 50/50 benzene/toluene mixture. The required purity are 95% for the distillate and 5% for the bottoms, respectively.

Powell's routine (see appendix A) is applied to minimize the total entropy productions (4.12) and (4.18). Like in chapter 3, random temperature profiles are used as initial guesses for the optimizations. It was observed that the convergence of the algorithm is slower for larger g-values. For large g-values the $\sum q_n^2$ term starts to dominate the behavior of equations (4.12) and (4.18). In this case the objective function converges rather slow, like the conventional column (3.7) which also contains a $\sum q_n^2$ term.

4.2.1 Influence of Heat Transfer Law

The optimal temperature profiles and corresponding heating requirements are determined for a 25-tray column with Fourier heat conduction (figures 4.1 and 4.2) and Newtonian heat conduction (figures 4.3 and 4.4). The three curves in each frame are calculated for $g = 0$ and for two increasingly severe transfer resistances. The value of zero represents perfect heat conduction and is therefore identical to the previous studies of optimal distillation considering only internal losses. The intermediate value corresponds to realistic heat conductance in a commercial heat exchanger, while the largest value of g is included to show the strongly resistive regime. The values of g_{NL} and g_{FL} are chosen to correspond to roughly the same temperature differences across the conductances and thus differ by a factor of $1.4 \cdot 10^5$ K^2 due to the forms of the two transfer equations (4.13) and (4.6). It is clear that the form of the transfer law has very little effect on the optimal temperature sequence and hence the heating demand. This speaks in favor of using the simpler Fourier expression (4.12) for the entropy production where temperature appears only in the heating terms, not in connection with the heat exchangers.

A further comparison between the two heat transfer laws is provided by figure 4.5, a log-log plot of the total entropy production relative to reversible heat transfer for a variation of g_{NL} and g_{FL} over 6 orders of magnitude. The realistic value of $g_{\mathrm{NL}} = 3 \cdot 10^{-4}$ moleK/J also used in figures 4.1–4.4 and the corresponding g_{FL} are marked on the curves. The two curves are remarkably similar. We see that heat resistance is insignificant for $g < 10^{-5}$ and dominant for $g > 10^{-3}$ with normal operation right in the middle of the transition interval. The type of heat transfer (Newtonian or Fourier) is immaterial.

4.2.2 Influence of Different Column Length

Figure 4.6, 4.8 and 4.10 show the optimal heating demands for columns with 25, 45 and 65 trays using Fourier heat conduction. As indicated in the previous subsection the corresponding Newtonian results are indistinguishable and are therefore not shown here. The shorter column displays the characteristic (inverted-u)-u shape of the heating curves observed in the last chapter for near reversible heat exchange. This is quickly smoothed out with increasing heat resistance where the internal losses, relatively speaking, become less significant.

The longest column by contrast, even for very slight heat resistance is oper-

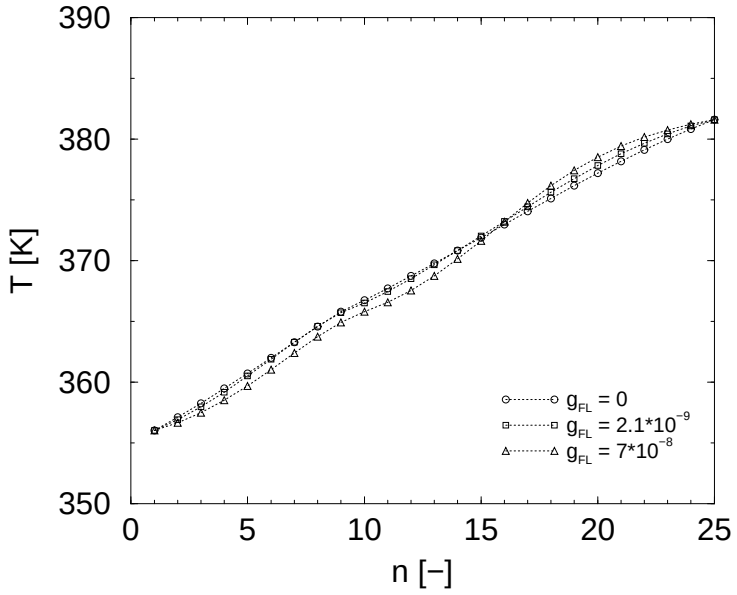

Figure 4.1: Optimal temperature profiles for a 25 tray column with a Fourier heat law connecting the heat exchangers to the supply fluids. The relative flow parameter g_{FL} is as indicated on the figure.

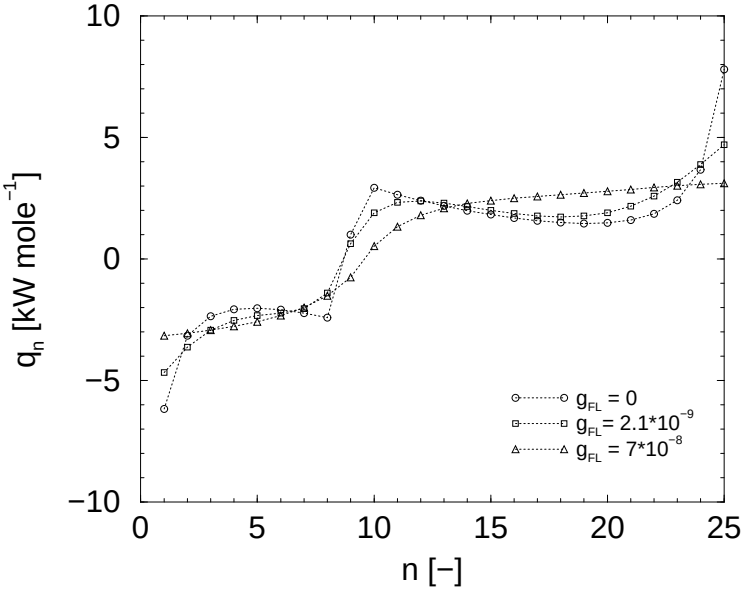

Figure 4.2: Corresponding optimal heating profiles

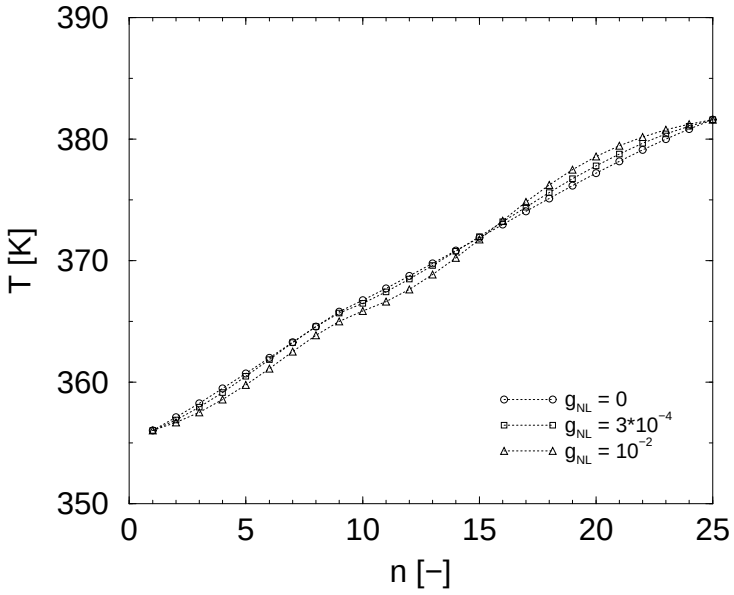

Figure 4.3: Optimal temperature profiles for a 25 tray column with a Newton heat law connecting the heat exchangers to the supply fluids. The relative flow parameter g_{NL} is as indicated on the figure.

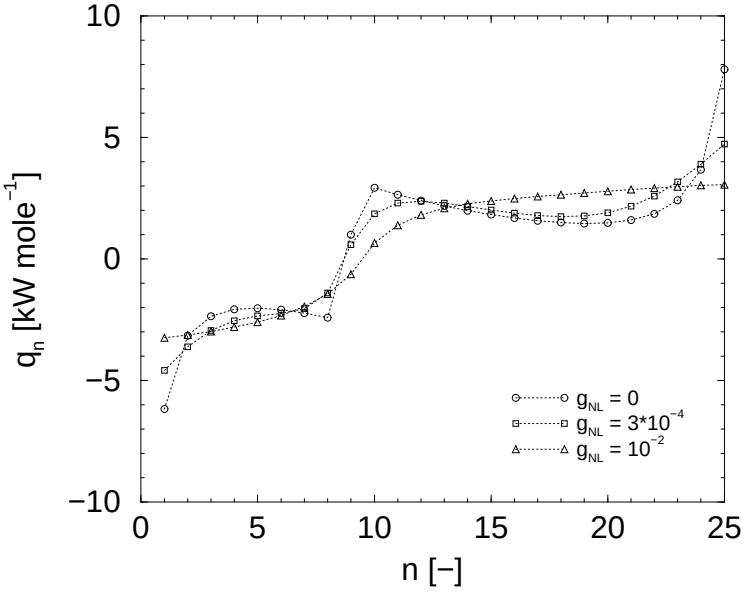

Figure 4.4: Corresponding optimal heating profiles

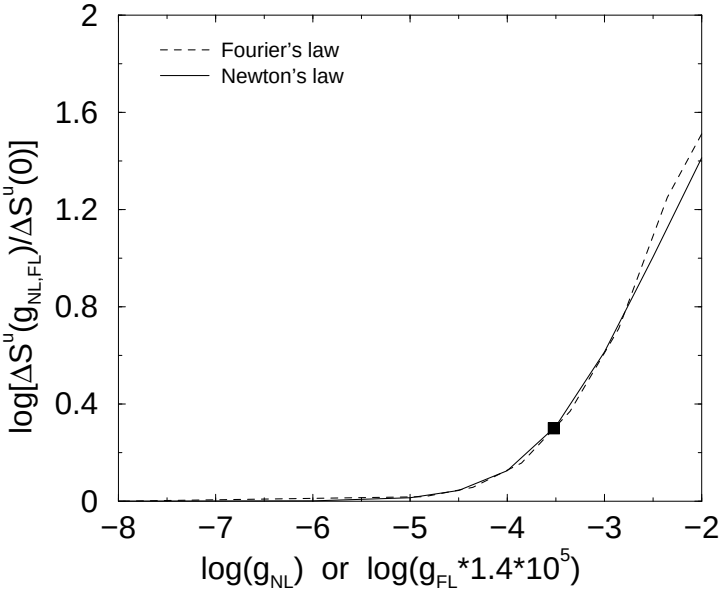

Figure 4.5: Log-log plot of the total entropy production relative to reversible heat transfer for a variation of g_{NL} and g_{FL} over 6 orders of magnitude. The point marked corresponds to industrially realistic values of heat conductance.

ated optimally with an essentially flat heating profile; the same rate of heat transfer on every tray in each section of the column. This resistive effect is quite surprising, quickly washing out the structure of the optimal unconstrained column. It promises well for the simplified diabatic column design advocated by Rivero [30, 32] in which the external heat exchange medium is passed in sequence through heat exchangers on one tray after another in the stripping and rectifying sections, respectively. This design obviously alleviates the need for costly independent heat supply circuits for each tray. At the same time all heating curves show a marked reduction in heat duty for the reboilers and condensers, making it possible to include them inside the column rather than as separate exterior units.

The corresponding curves for the entropy production on each tray are even more illuminating for the effect of heat resistance. The entropy production due to heat and mass transfer on the trays alone is by no means flat, rather it follows the general shape originally developed in interior optimization. The entropy production due to heat exchange, is not flat either, but together the internal and external entropy productions add up to an almost constant entropy production on each tray, a kind of equipartition often claimed to be a good design principle [39]. Optimal heat exchange on the feed tray is

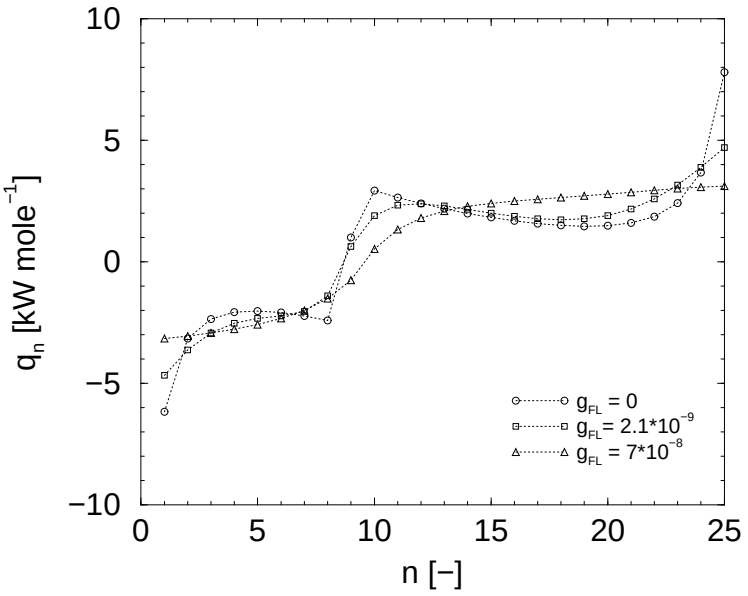

Figure 4.6: Optimal heat duties for the individual trays in a 25 tray column with a Fourier heat transfer. The relative flow parameter g_{FL} is as indicated on the figure.

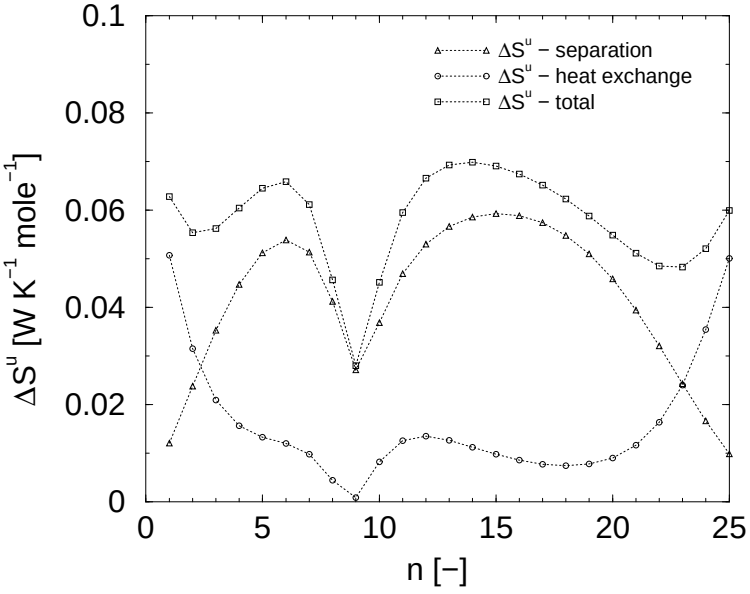

Figure 4.7: Optimal distribution of entropy production on the individual trays for a 25 tray column. Here $g_{\mathrm{FL}} = 2.1 \cdot 10^{-9}$ mole/JK (industrially realistic value).

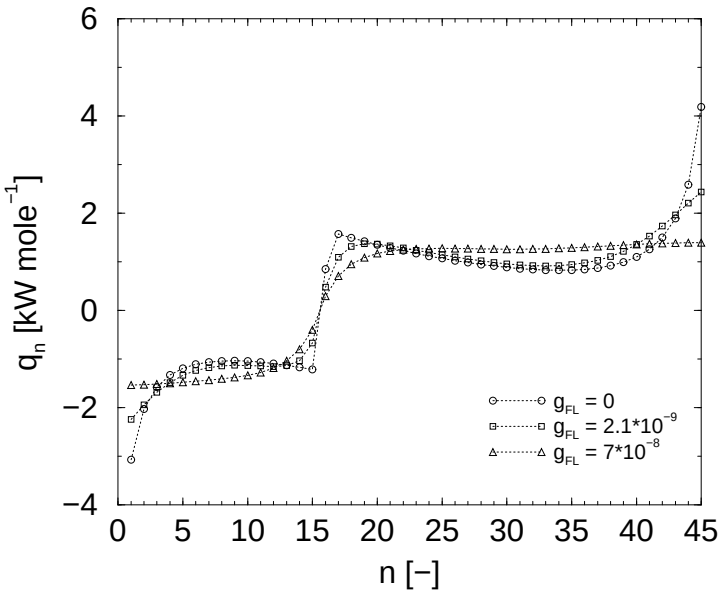

Figure 4.8: Optimal heat duties for the individual trays in a 45 tray column with a Fourier heat transfer. The relative flow parameter g_{NL} is as indicated on the figure.

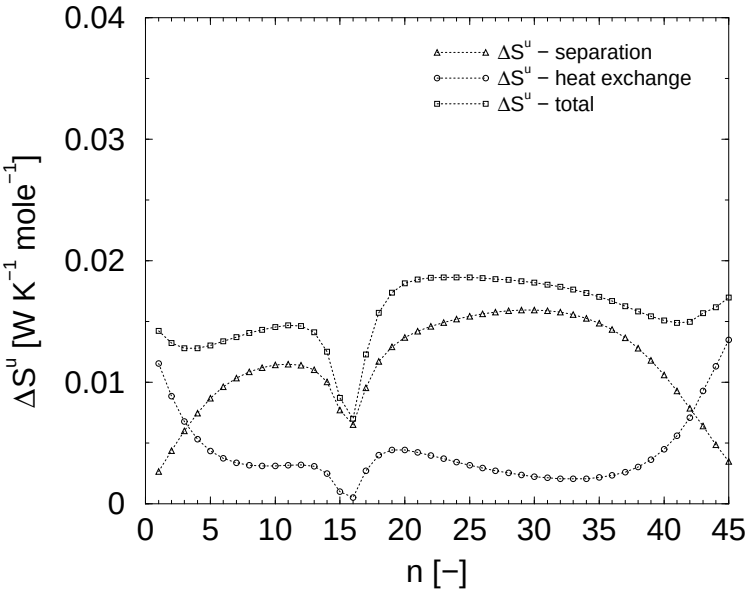

Figure 4.9: Optimal distribution of entropy production on the individual trays for a 45 tray column. Here $g_{\mathrm{FL}} = 2.1 \cdot 10^{-9}$ mole/JK (industrially realistic value).

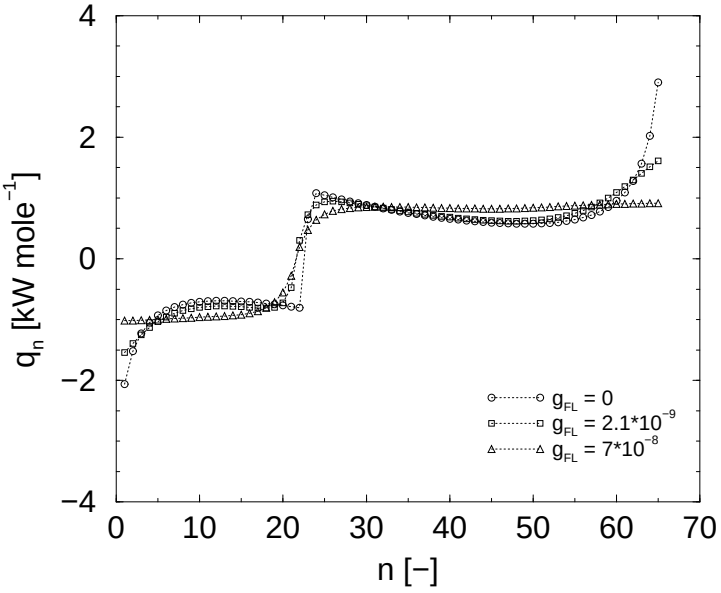

Figure 4.10: Optimal heat duties for the individual trays in a 65 tray column with a Fourier heat transfer. The relative flow parameter g_{NL} is as indicated on the figure.

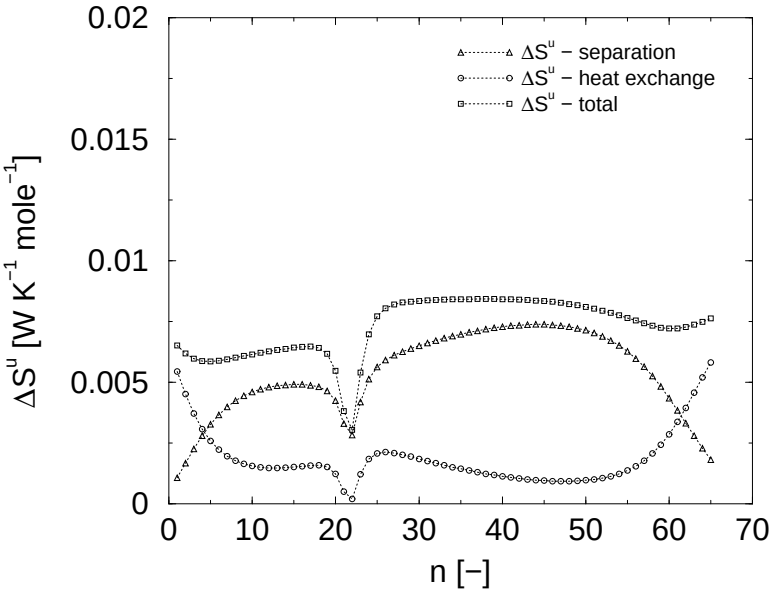

Figure 4.11: Optimal distribution of entropy production on the individual trays for a 65 tray column. Here $g_{\mathrm{FL}} = 2.1 \cdot 10^{-9}$ mole/JK (industrially realistic value).

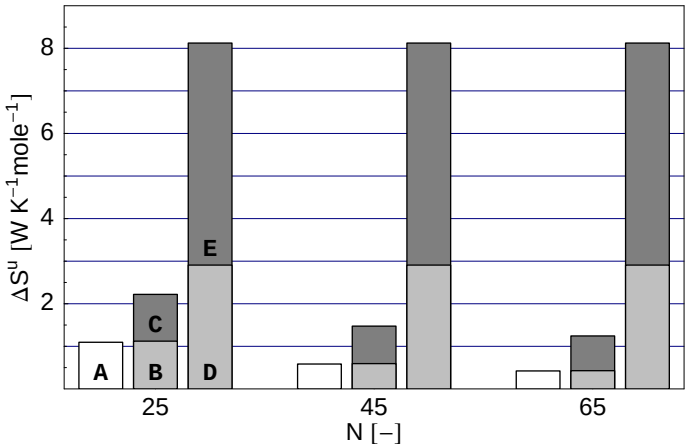

Figure 4.12: Entropy production in adiabatic and diabatic columns of length 25, 45 and 65 trays. The leftmost histogram (A) shows the ultimate lower limit for a diabatic column with $g = 0$. The center histogram shows the entropy production due to the internal heat and mass flows (B), the heat exchange (C) for a diabatic column with $g_{\mathrm{FL}} = 2.1 \cdot 10^{-9}$ mole/JK. The right histogram shows the separation (D) and heat exchanger losses (E) for a corresponding conventional adiabatic column.

usually quite small and can be made zero by appropriately balancing of the vapor/liquid composition in the feed.

The entropy savings by using a diabatic column compared to a conventional adiabatic one are evident from figure 4.12. Even for the shortest column of 25 trays, the adiabatic entropy production (including heat exchanger losses) is four times as large as the losses in the diabatic column, with the heat exchangers accounting for about two thirds of the losses. In the diabatic column, the contribution of heat exchange varies from about half for the shortest column to about two thirds for the longest column. To indicate the ultimate lower limit of entropy production without regard to heat exchange losses, the curve for $g = 0$ is shown as the leftmost histogram.

4.3 Summary

In the absence of counting heat transfer irreversibilities due to heat exchange between column and its surroundings, the optimal heating profile is independent of rate of operation in the sense that the optimal heating profile scales directly with the feed rate. This is no longer the case once the irreversibilities

of the heat coupling to the outside of the column are included. For slow operation (small g-values) the solution is essentially unchanged from the solution for the problem without irreversibilities due to the heat transfer. For fast operation (large g-values) the entropy production inside the column becomes negligible compared to the irreversibilities due to the heat exchange which then dominate the behavior of the optimum. The optimal heating profiles smooth out with increasing heat resistance. Particularly, long columns are optimally operated with essentially flat heating profiles.

For industrially relevant g-values, the entropy production of an adiabatic column (including heat exchanger losses) is several times larger than the entropy production in the optimized diabatic column. The contribution of the heat exchange to the entropy production increases with column length. The results from chapter 3 as well as the extended study including heat transfer irreversibilities in this chapter reveal that the simplified diabatic column design suggested by Rivero [30] is a promising attempt to implement diabatic distillation columns.

The results of this chapter have been published in [48].

Chapter 5

Sequential Heat Exchangers

In the previous two chapters we found the minimum irreversibility for diabatic distillation cloumns, where each tray was supplied by *independently adjustable* heat exchangers. However, such a design could be difficult to implement in practise. For each tray, two piercings in the column containment are required, and each tray needs an individual heat exchange circuit. These extra investment costs may outbalance the savings achieved by reducing the exergy losses.

Rivero [30] proposed a simplified diabatic column design which is particular suitable for retrofitting applications and therefore more promising than a diabatic column with independently controlled tray temperatures. The Rivero implementation uses a single heating fluid circulating in series from one tray to the next below the feed tray and a single cooling fluid circulation in series above the feed tray, as shown in figure 5.1.

Such a sequential heat exchanger design has only four control variables:

1. The temperature of the sequential heat exchanger fluid entering the rectifier.
2. The flow rate of the sequential heat exchanger fluid in the rectifier.
3. The temperature of the sequential heat exchanger fluid entering the stripper.
4. The flow rate of the sequential heat exchanger fluid in the rectifier.

The temperature profile of the distillation column is determined by these four parameters.

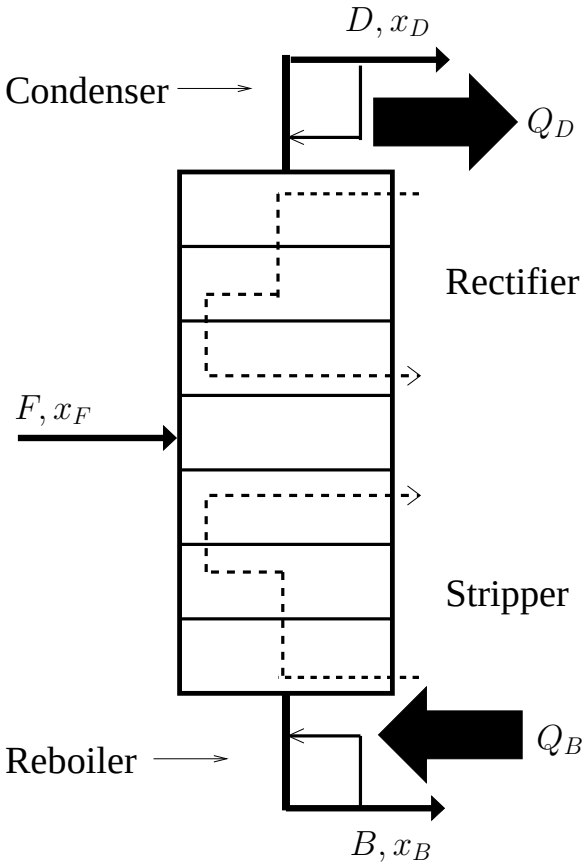

Figure 5.1: Conventional column retrofitted with sequential heat exchangers as proposed by Rivero. The sequential heat exchanger fluid flow is indicated by the dashed lines.

In this chapter, numerical optimization is used to determine the optimal operation of a diabatic design with sequential heat exchangers. In particular, we focus on how much extra irreversibility one has to pay for the loss of independent control of the external temperatures.

5.1 Heat Exchanger Model

Consider first a model of a heat exchanger on a single tray (see figure 5.2), where the heat exchanger model is taken from standard thermal engineering literature, e.g. [14, 15]. Let $\dot{m}$ be the flow rate of the heat exchanger fluid, $T_{\mathrm{ex},1}^{\mathrm{in}}$ and $T_{\mathrm{ex},1}^{\mathrm{out}}$ be the temperatures of the heat transfer fluid coming in and

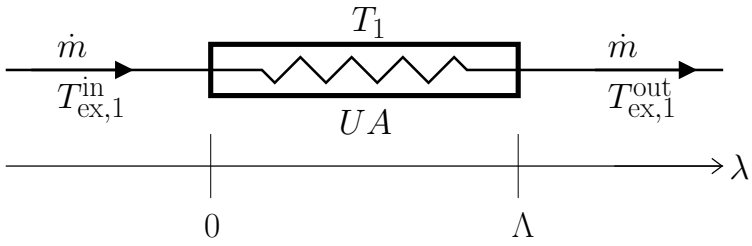

Figure 5.2: Model of a single heat exchanger on one tray. The spatial parameter λ runs from 0 to Λ.

going out of the tray, T_1 be the temperature of the tray, c_p be the specific heat capacity of the heat transfer fluid, Λ be the length of the contact area of the heat exchanger, λ be the position along the heat exchanger, and UA be the product of the heat exchanger area A and the heat conductivity U giving the total conductance of the heat exchanger unit. For convenience, the flow rate $\dot{m}$, and thermal properties c_p and UA are assumed to be temperature independent.

The heat flow in a small portion $\mathrm{d}\lambda$ is then

$$\dot{m}c_\mathrm{p}\mathrm{d}T_{\mathrm{ex},1} = -\frac{UA}{\Lambda}(T_{\mathrm{ex},1} - T_1)\mathrm{d}\lambda. \tag{5.1}$$

Separating variables and integrating along the length of the heat exchanger gives

$$\int_{T_{\mathrm{ex},1}^{\mathrm{out}}}^{T_{\mathrm{ex},1}^{\mathrm{in}}} \frac{\mathrm{d}T_{\mathrm{ex},1}}{(T_{\mathrm{ex},1} - T_1)} = -\frac{UA}{\dot{m}c_\mathrm{p}\Lambda}\int_0^\Lambda \mathrm{d}\lambda. \tag{5.2}$$

Solving the resulting equation results in

$$T_{\mathrm{ex},1}^{\mathrm{out}} = T_{\mathrm{ex},1}^{\mathrm{in}} + (T_1 - T_{\mathrm{ex},1}^{\mathrm{in}})\left[1 - \exp\left(-\frac{UA}{\dot{m}c_\mathrm{p}}\right)\right]. \tag{5.3}$$

The rate of heat transferred in the heat exchanger is given by

$$Q_1^{\mathrm{hx}} = \dot{m}c_\mathrm{p}(T_{\mathrm{ex},1}^{\mathrm{in}} - T_1)\left[1 - \exp\left(-\frac{UA}{\dot{m}c_\mathrm{p}}\right)\right], \tag{5.4}$$

and the entropy production associated with the heat transfer is calculated as

$$\Delta S_1^{\mathrm{u,hx}} = \dot{m}c_\mathrm{p}\ln\left(\frac{T_{\mathrm{ex},1}^{\mathrm{out}}}{T_{\mathrm{ex},1}^{\mathrm{in}}}\right) + \frac{Q_1}{T_1}. \tag{5.5}$$

Figure 5.3 shows a schematic representation of a serial heat exchanger meandering through n trays. Using equation (5.3) and knowing the temperatures

of the trays and the flow rate of the heat exchange fluid entering the sequential heat exchangers, the amount of heat transferred can be calculated at each tray along the heat exchanger.

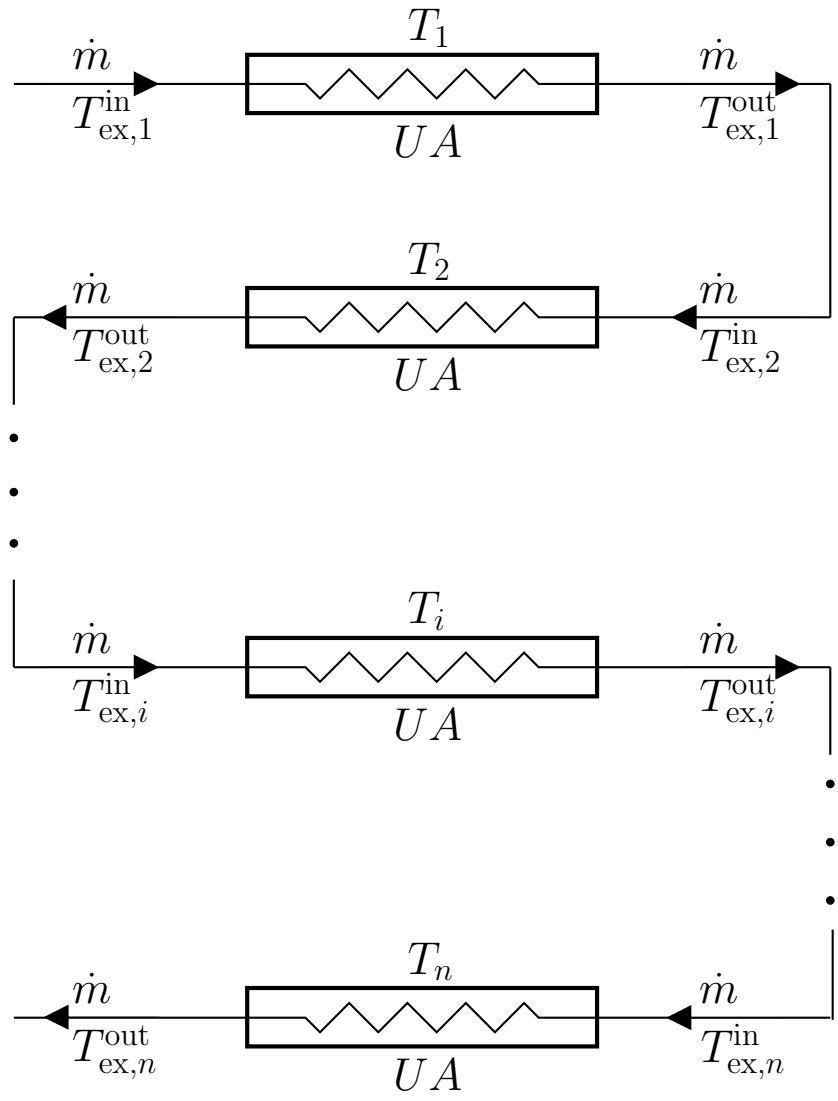

Figure 5.3: Serial heat exchanger meandering through tray 1 to tray n of the distillation column

5.2 Computational Method

The heating stream of the sequential heat exchanger design enters the stripper section of the column at tray $N-1$ with a mass flow rate $\dot{m}_{\mathrm{B}}$ and a temperature of $T^{\mathrm{in}}_{\mathrm{ex,B}}$, and leaves the column one tray below the feed tray at a temperature $T^{\mathrm{out}}_{\mathrm{ex,B}}$. The cooling stream enters the rectifier section at tray 1 with a mass flow rate $\dot{m}_{\mathrm{D}}$ and a temperature of $T^{\mathrm{in}}_{\mathrm{ex,D}}$, and leaves the column one tray above the feed tray at a temperature $T^{\mathrm{out}}_{\mathrm{ex,D}}$. Feed tray, reboiler, and condenser are not supplied by the seqential heat exchanger fluid.

Our aim is to find the optimal heat exchanger fluid parameters ($\dot{m}_{\mathrm{B}}$,$\dot{m}_{\mathrm{D}}$, $T^{\mathrm{in}}_{\mathrm{ex,B}}$, $T^{\mathrm{in}}_{\mathrm{ex,D}}$) to achieve minimal entropy production.

5.2.1 Entropy Production and Steady State Condition

With equation (2.21) for the entropy production associated with the separation process inside the column, and summing up expression (5.5), over all trays supplied by the heat exchanger fluid, the overall entropy production for the sequential heat exchanger design is

$$\begin{aligned}\Delta S^{\mathrm{u}}(\dot{m}_{\mathrm{B}}, \dot{m}_{\mathrm{D}}, T^{\mathrm{in}}_{\mathrm{ex,B}}, T^{\mathrm{in}}_{\mathrm{ex,D}}) &= \dot{m}_{\mathrm{B}}\, c_{\mathrm{p,B}} \ln\left(\frac{T^{\mathrm{out}}_{\mathrm{ex,B}}}{T^{\mathrm{in}}_{\mathrm{ex,B}}}\right) + \dot{m}_{\mathrm{D}}\, c_{\mathrm{p,D}} \ln\left(\frac{T^{\mathrm{out}}_{\mathrm{ex,D}}}{T^{\mathrm{in}}_{\mathrm{ex,D}}}\right) \\ &+ \Delta S^{\mathrm{B}} + \Delta S^{\mathrm{D}} + \Delta S^{\mathrm{massflows}}. \end{aligned} \tag{5.6}$$

Here ΔS^{B} and ΔS^{D} denote the entropies entering reboiler and condenser, respectively. Equation (5.6) holds for steady state condition, when the column temperature profile is such that the heat duty (2.8) on each tray n of the column matches the heat (5.4) delivered by the heat exchanger fluid on that tray,

$$Q_n = Q^{\mathrm{ex}}_n, \qquad n = (2, \ldots, N-1). \tag{5.7}$$

This steady state condition has to enter the optimization problem as an additional constraint for the tray temperatures. In principle, the constraint can be added to the entropy production (5.6) as penalty function of the form $\mathcal{P} = M \sum_n (Q_n - Q^{\mathrm{ex}}_n)^2$, where M is a large constant.

Unfortunately, standard minimization methods applied to this penalized objective function fail to find a minimum as the procedure invariably gets stuck. This is due in part to the fact that this is a simulation where only narrow regions of parameter values make physical sense. It is further complicated

by numerous local minima and by the high sensitivity of the entropy production on the temperature profile. Therefore a different approach based on an algorithm using a pseudo-dynamic is developed for finding the steady state temperature profile.

5.2.2 Pseudo-dynamic Algorithm

In each iteration of the minimization procedure with respect to the control vector $\mathbf{v} = (\dot{m}_{\mathrm{B}}, \dot{m}_{\mathrm{D}}, T^{\mathrm{in}}_{\mathrm{ex,B}}, T^{\mathrm{in}}_{\mathrm{ex,D}})$, we have to find the corresponding steady state temperature profile for the current value of $\mathbf{v}$. Since the operating characteristics of the column are conveniently expressed in terms of its temperature profile $\mathbf{T}$, it is natural to start the search for the steady state profile by guessing an initial temperature profile.

We define the vector of deviation from the steady state condition (5.7) by

$$\mathbf{Q}^{\mathrm{excess}}(\mathbf{T}, \mathbf{v}) := \mathbf{Q}^{\mathrm{ex}}(\mathbf{T}, \mathbf{v}) - \mathbf{Q}(\mathbf{T}, \mathbf{v}). \tag{5.8}$$

Further we evaluate the error expression

$$\epsilon = \mathbf{Q}^{\mathrm{excess}} \cdot \mathbf{Q}^{\mathrm{excess}}, \tag{5.9}$$

Now the temperature of each tray is changed by a small multiple δ of the excess heat on that tray according to a discrete pseudo-dynamics,

$$\mathbf{T}(t+1) = \mathbf{T}(t) + \delta \mathbf{Q}^{\mathrm{excess}}(t), \tag{5.10}$$

where t denotes the 'time' iteration.

Starting with the initially guessed temperature profile, (5.8)-(5.10) are evaluated iteratively. The error evaluation allows us to adjust the size of δ in each ireration. If the error ϵ of one iteration is bigger than the one of the previous iteration, δ ist reduced by an empirical factor, whereas δ is slightly increased if ϵ becomes smaller.

This heuristic scheme converges to the steady state temperature profile for the current value $\mathbf{v}$ in the main optimization routine.

5.3 Optimization Results

The examples presented here use a conductance $UA = 500\,\mathrm{W/K}$ on each tray and ten times this value for the reboiler and the condenser. The specific heat

capacity of the heat exchange fluid used is the same for both the rectifier and stripper section, and is taken to be $c_{\mathrm{p}} = 300\,\mathrm{J\,(K\,mole)^{-1}}$. The calculations compare a 20 tray diabatic column and a 20 tray adiabatic column, both separating an ideal 50/50% benzene/toluene mixture to yield a purity of 95% distillate and 5% bottoms. The results discussed include

- the heating and cooling duties
- the tray-by-tray entropy production
- liquid and vapor flow rates
- the temperature profiles
- the sensitivity of entropy production as the heat transfer fluid inlet temperatures deviates from their optimal values
- the amount of exergy savings compared to an adiabatic column
- and the minimum entropy production as a function of the total number of trays

5.3.1 Operation Profiles

The left graph in figure 5.4 shows the heating and cooling duties for a sequential heat exchanger column and its conventional counterpart. It turns out that since the sequential heat exchangers reduce the duty that the reboiler and condenser must perform, a diabatic column with these parameters requires a reboiler that is only half the size of a conventional column and a condenser 2/3 the size of a conventional column. As already found in our previous studies, the heating and cooling loads are essentially constant over the trays.

Figure 5.4 shows that the total entropy production rate is significantly lower in the diabatic column and that it is more uniformly distributed; only the feedtray deviates noticeably. This indicates that all the trays carry more or less the same burden of separation, quite distinct from the performance in the adiabatic column. When comparing the entropy production of the condensers (tray 0), it is observed that the entropy production in the adiabatic column's condenser is approximately twice as large as the corresponding entropy production in the diabatic column. Similarly, the entropy production in the adiabatic column's reboiler (tray 20) is four times larger than the entropy production of the diabatic column's reboiler.

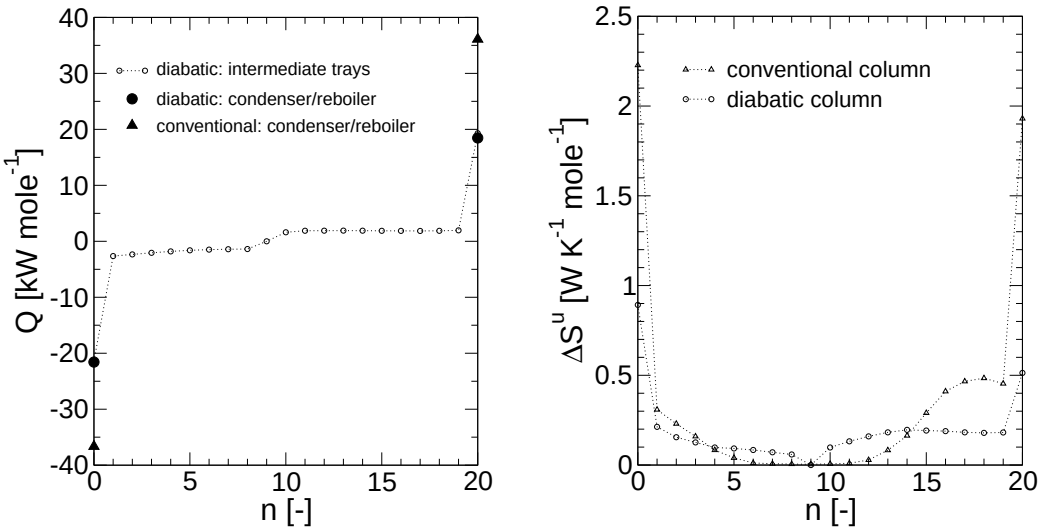

Figure 5.4: Heating and cooling duties (left) and entropy production per tray (right) for a 20 tray sequential heat exchanger column.

Except for the feed tray, the diabatic column flow rates are noticeably lower than those of the adiabatic column as seen in figure 5.5. The significance of lower flow rates is that the column allows cross sectional area for the serial heat exchangers to be installed without interfering with the material flows in the column, implying that a conventional column can be retrofitted with the serial heat exchangers without adverse effects.

In figure 5.6 the middle solid line of the diabatic column chart shows the temperature of each tray in the column; the line below the middle line is the temperature profile for the sequential heat exchangers in the rectifier, while the one above is the temperature profile for the sequential heat exchanger in the stripper. As for all optimized diabatic columns, the tray temperatures vary almost linearly along the column, indicating that each tray is doing its share of the separation process. The heat exchanger temperatures are roughly a constant difference away from the tray temperatures, again indicating a uniform dissipation. By contrast the adiabatic column has very little temperature change across trays 7 through 12. Thus the serial heat exchangers help the diabatic column to utilize the trays better.

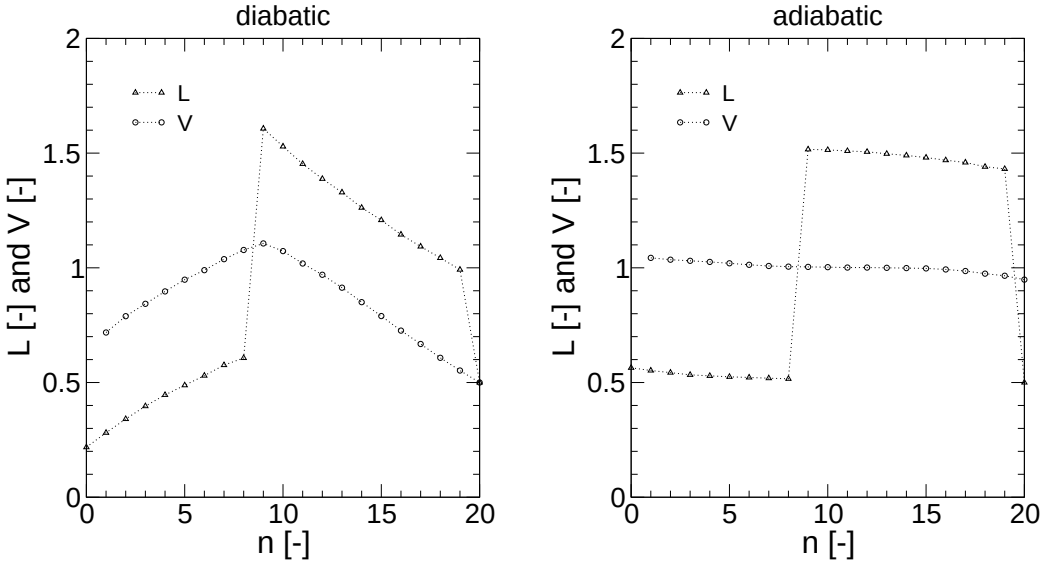

Figure 5.5: Liquid and vapor flow profiles for a diabatic column with sequential heat exchangers and a adiabatic reference column.

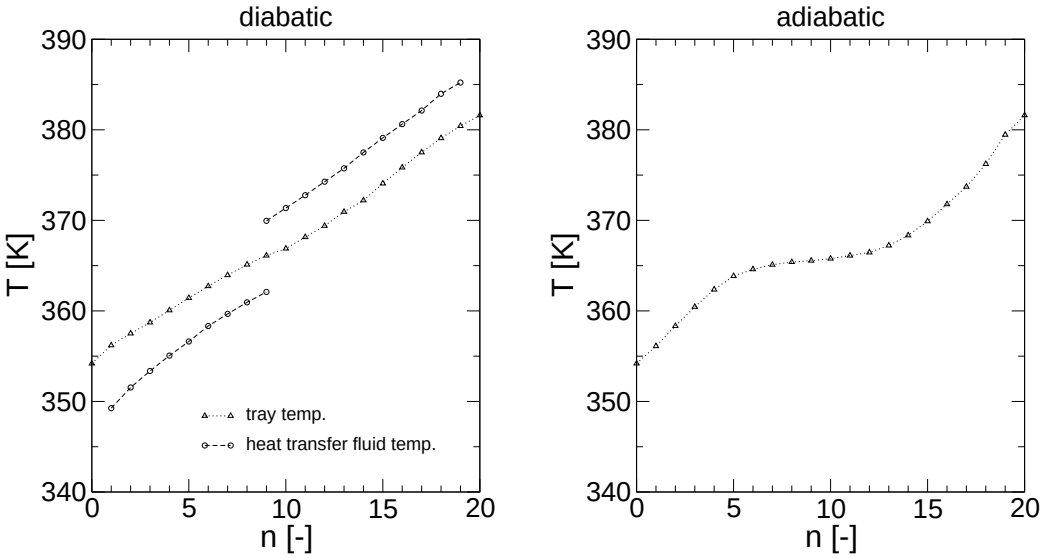

Figure 5.6: Temperature profiles for a diabatic column with sequential heat exchangers and a adiabatic reference column.

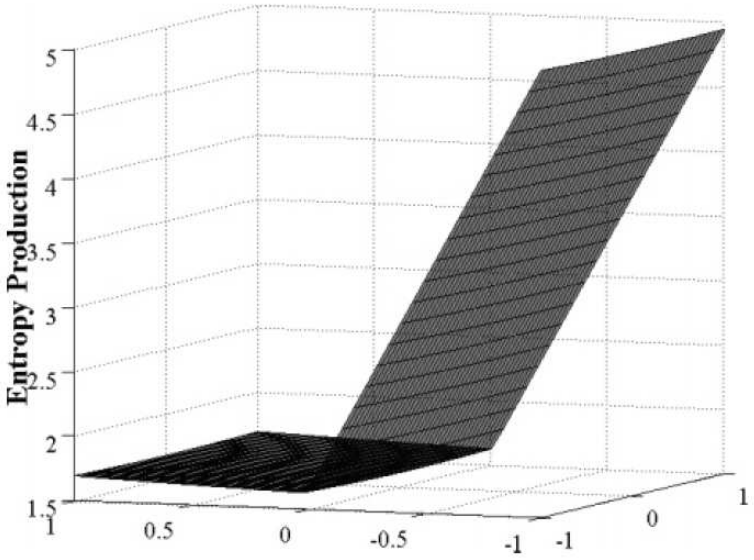

Figure 5.7: Sensitivity of entropy production rate as a function of deviations from the optimal heat exchange fluid inlet temperatures.

5.3.2 Total Entropy Production

In order to investigate the sensitivity of the column performance on the four control parameters (two mass flowrates and two inlet temperatures) of the serial heat exchangers, the following experiment was conducted. Varying either optimal inlet temperature by one Kelvin in the direction away from the feedpoint (i.e. slightly larger driving force) will result in an entropy production increase of approximately 15%, while varying either temperature toward the feedpoint will yield an entropy production increase of 400%. The reason for the latter is a strongly increasing demand on the reboiler and condenser when the serial heat exchangers have a smaller driving force and thus exergetically less efficient operation.

Figure 5.8 shows the potential efficiency improvements by using a diabatic column with serial heat exchange instead of a traditional adiabatic column for the separation process at hand for different length columns. At the short end a 15 tray column achieves 35% smaller entropy production rate while at the high end a 40 tray column can conserve more than two thirds of the losses, 69%. Generally, the more trays a diabatic column has, the greater the savings, eventually approaching reversible separation for a column of infinite length. Even when the heat exchanger conductance is reduced to half, the improvements are still 32% and 67%, respectively.

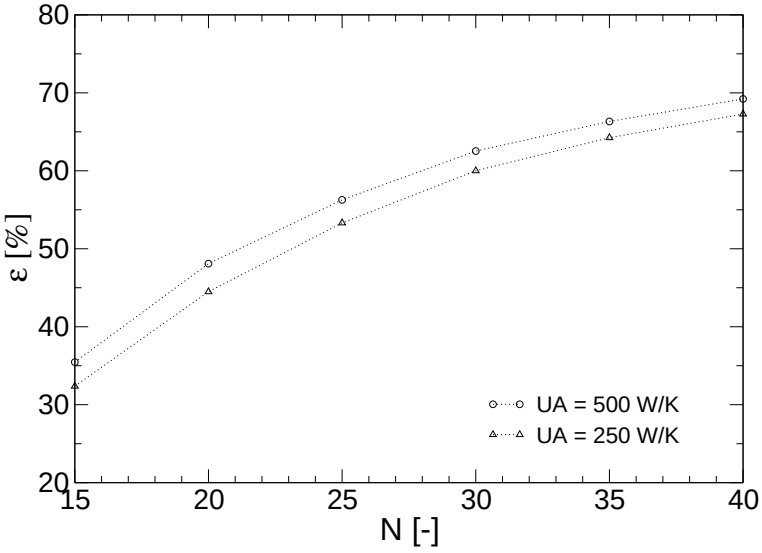

Figure 5.8: Percent savings ε of entropy production of a diabatic column with sequential heat exchange versus an adiabatic column of the same length for two different heat conductances.

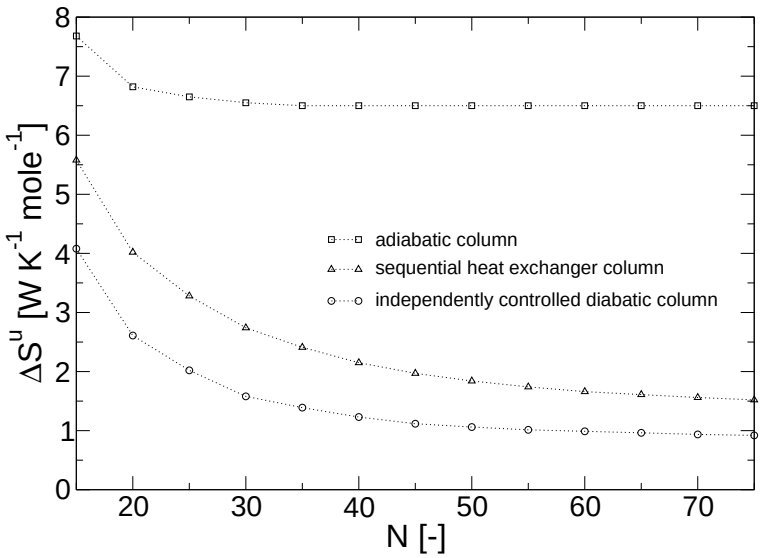

Figure 5.9: Entropy production rate comparison between an adiabatic column, an independently controlled diabatic column, and a diabatic column with sequential heat exchangers.

Finally, in figure (5.9) we compare the entropy production rates for fully diabatic columns, columns with serial heat exchange, and adiabatic columns over a range of lengths. First of all the savings in using a diabatic column are substantial, the more so the longer the column. We also see that there is a price for giving up the total freedom of optimizing the heat exchange on each tray individually and installing serial heat exchangers instead, but it is fairly small, especially for the longer columns. Considering the technical advantages of the serial heat exchange scheme – only four piercings of the column containment rather than two for each tray, and the need for only one heat source and one cold source rather than one for each tray – makes this design most suitable for retrofitting distillation columns.

5.4 Summary

One particular implementation of diabatic clolumns uses a single cooling fluid circulating in series from one tray to the next above the feed tray and one heating fluid circulating in series below the feed. Minimizing the overall entropy production rate for such a sequential heat exchanger installation has shown to be a difficult task as standard minimization procedures get stuck unlike in the case of independently controlled tray temperatures. This problem was solved by applying a heuristic algorithm based on physical intuition for adjusting the column temperature profile. The optimal operating profiles do not differ significantly from the ones obtained for the indepently controlled column. For the latter the reduction in entropy production is moderately higher compared to the sequential heat exchanger design, which is convincing because of its retrofitting suitability. The results in this chapter are published in [49, 50].

Chapter 6

Conclusions

Contrary to conventional distillation, in diabatic distillation columns additional heat exchange is allowed on all trays inside the column. Diabatic distillation produces significantly less entropy than adiabatic distillation, since the input heat can be on average colder and the rejected heat can be on average warmer.

In this work the optimal diabatic operation is found by numerically minimizing the entropy production for sample columns separating an ideal benzene/toluene mixture. In the first investigation, we focused on the entropy production inside the column due to internal heat and mass transfer. For high purity requirements and diabatic columns with many trays we found a tremendous reduction of entropy production. A comparison of the numerical results with results obtained from the asymptotic ETD theory revealed a surprisingly good agreement for large number of trays. The optimal diabatic temperature profiles show that the separation is distributed more evenly along the column. For long columns, the heating or cooling duties tend to be roughly the same for each tray. Most important, reboiler and condenser duties are significantly smaller than in a conventional column.

In a second investigation, the irreversibility arising from the heat coupling of the column to its surroundings is included in the total entropy production. With increasing heat resistance the optimal heat duty profiles smooth out. Particularly, long columns are optimally operated with essentially flat heating profiles. The contribution of the heat exchange to the overall entropy production increases with column length. Also with inclusion of heat exchanger losses, we still find enormous savings in entropy production compared to a conventional reference column.

The sequential heat exchanger column with one single cooling circuit in the

rectifier and one single heating circuit in the stripper section is analyzed with a heuristic algorithm using a pseudo-dynamic representation of the column temperature profile. Remarkably, the amount one has to pay for reducing the number of control variables to four is fairly small. Thus, this particular implementation is most convincing, besides its retrofitting suitability.

Undoubtedly, diabatization has shown to be promising concept to increase efficiency of distillation. However, there are some potential issues for further investigation:

Regarding the optimal allocation of a fixed total heat exchanger inventory in the diabatic column, additional investigations have to be carried out. A first study was done by Jimenez *et al.* [51], who introduced a fifth control variable to the sequential heat exchanger model. This extended optimization showed that the longer the column, the less heat exchanger inventory should be allotted to the trays. Other approaches (Koeijer *et al.* [52]) also found a significant effect of the heat exchanger inventory on the entropy production.

Basically, diabatic distillation is still a theoretical concept. Only Rivero [30] has done an extensive experimental study on an diabatic pilot plant so far. As a result, theoretical predictions for diabatic columns are experimentally confirmed [53]. More experimental studies would be necessary to gain a comprehensive insight of how diabatic columns work under realistic conditions. In addition, future theoretical work must inlcude nonidealites, e.g. realistic tray efficiencies.

Apart from the straightforward diabatization by adding heat exchangers to the trays, there is a different promising concept – the pressure swing column – under discussion. It goes back to Mah [54] who analyzed a distillation model with different pressures in the rectifying and stripping section. This makes it possible to add the heat that is removed in the rectifier to the stripper. Comparative studies regarding the savings achieved with such an installation and with the diabatic types in the present work is another possible future research topic.

Despite the potential exergy savings in diabatic columns, their application eventually depends on economical considerations. Capital costs are reduced due to the smaller size of reboiler and condenser in diabatic column, but are increased by additional heat exchanger inventory and more trays. The operation costs are expected to decrease due to the smaller heat duties especially at reboiler and condenser. Whether these facts are sufficient for a potential broad application is an open issue and beyond the scope of this work.

Appendix A

Standard Optimization Methods

Throughout this thesis standard optimization methods are applied to the minimization of the entropy production. Primarily, Powell's algorithm [46] is used for the optimization, while the downhill simplex method is used to countercheck and confirm the results as well as to optimize the sequential heat exchanger column with respect to the heat transfer fluid parameters.

A.1 Powell's Method

Consider a function $f(\mathbf{x})$, $\mathbf{x} = (x_1, \ldots, x_N)$ to be minimized. The main idea of Powell's method for achieving convergence is by searching down a given set of search directions $\mathbf{U} = (\mathbf{u}_1, \ldots, \mathbf{u}_N)$ with each element updated iteratively. This produces N mutually conjugate directions which means that once all elements of the direction set are linearly independent, the next N line minimizations will put the function at its minimum. This is true for quadratic forms; for functions that are not exactly quadratic forms, it won't be exactly the minimum, but repeated cycles of N line minimizations (one dimensional minimization along one particular direction) will converge quadratically to the minimum. The proof for quadratic convergence is given in [46].

Unfortunately, Powell's quadratically convergent method tends to produce sets of search directions that are linearly dependent. In [55] a modified Powell algorithm is presented that avoids this problem. For this version one has to give up quadratic convergence, but for functions with long, twisty

valleys (like the entropy productions (3.3), (3.7), (4.18) and (4.12)) quadratic convergence is of no particular advantage.

The minimization algorithm consists of the following steps:

1. Choose a starting position and save it as $\mathbf{P}_0$ and initialize the search directions $\mathbf{u}_i$ to the basis vectors of the $\mathcal{R}^N$, i. e. $\mathbf{u}_i = \mathbf{e}_i$, $i = 1, \ldots, N$.

2. Repeat the following procedure until the function stops decreasing:

   - For each direction $\mathbf{u}_i$, $i = 1, \ldots, N$, minimize along that direction using the $\mathbf{P}_{i-1}$ as starting point. Save the result as $\mathbf{P}_i$. The line minimization is performed by a bracketing routine and parabolic interpolation (Brent's method [55, 56]). Save direction $\mathbf{u}_L$ along which the function made its largest decrease Δf. Save the average direction moved $\mathbf{P}_N - \mathbf{P}_0$.
   - Define the quantities

     $$f_0 \equiv f(\mathbf{P}_0), \quad f_N \equiv f(\mathbf{P}_N), \quad f_E \equiv f(2\mathbf{P}_N - \mathbf{P}_0). \tag{A.1}$$

   - If one of the inequalities

     $$f_E \geq f_0 \quad \text{or} \quad \frac{2(f_0 - 2f_N + f_E)[(f_0 - f_N) - \Delta f)]}{\Delta f (f_0 - f_E)^2} \geq 1, \tag{A.2}$$

     holds, then keep the old direction set. Save $\mathbf{P}_N$ as $\mathbf{P}_0$. Go back for another iteration. If condition (A.2) does not apply, discard the direction of largest decrease $\mathbf{u}_L$ and assign $\mathbf{u}_L \leftarrow \mathbf{u}_N$. This avoids a buildup of linear dependence of the search directions. Assign $\mathbf{u}_N \leftarrow (\mathbf{P}_N - \mathbf{P}_0)$. Minimize along the new $\mathbf{u}_N$ and save the result as $\mathbf{P}_0$. Go back for another iteration.

A.2 Downhill Simplex Method

The downhill sipmlex method is due to Nelder and Mead [57]. Like Powell's procedure, it does not require gradient information. It is a relatively slow, but simple and robust algorithm. In N dimensions, a simplex is the geometrical figure consisting of $N + 1$ points and all their interconnecting line segments, polygonal faces, etc. For example, in two dimensions, a simplex is a triangle. In three dimensions, it is a – not necessarily regular – tetrahedron.

Basically, the algorithm consists of the following steps:

1. Define an initial simplex. The simplest way to do this is to choose an initial point $\mathbf{P}_0$ and to take the other N points to be $\mathbf{P}_i = \mathbf{P}_0 + \lambda \mathbf{e}_i$, where $\mathbf{e}_i$ are N unit vectors and where λ is a guess of the problem's characteristic length scale.

2. Evaluate the objective function for all points of the simplex. Determine the highest (worst), next highest, and lowest (best) point. Compute the fractional range from the highest to the lowest point and compare with required accuracy. If unsatisfactory, continue with next step.

3. Construct a new simplex volume by:

   (a) First reflect the simplex from the high point, i.e. extrapolate by a factor -1 through the face of the simplex across from the high point.

   (b) If the previous step gives a result better than the current best point, do an additional extrapolation along this direction by a factor 2.

   (c) Otherwise, if the reflected point is worse than the second highest, look for an intermediate point, which is done by an one-dimensional contraction by a factor 1/2.

   Go back to step 2, and repeat procedure until required accuracy is fulfilled.

Bibliography

[1] F. L. Curzon and B. Ahlborn. Efficiency of a carnot engine at maximum power output. *Am. J. Phys.*, 43:22–24, 1975.

[2] S. Sieniutycz and P. Salamon, editors. *Finite-Time Thermodynamics and Thermoeconomics*. Taylor and Francis, New York, 1990.

[3] R. S. Berry, V. A. Kazakov, S. Sieniutycz, Z. Szwast, and A. M. Tsirlin. *Thermodynamic Optimization of Finite-Time Processes*. John Wiley & Sons, Chicester, 2000.

[4] P. Salamon, J. D. Nulton, G. Siragusa, T. R. Andersen, and A. Limon. Principles of control thermodynamics. *Energy*, 26(3):307–319, 2001.

[5] M. H. Rubin. Optimal configuration of a class of irreversible heat engines. I. *Phys. Rev. A*, 19(3):1272–1276, 1979.

[6] M. H. Rubin. Optimal configuration of a class of irreversible heat engines. II. *Phys. Rev. A*, 19(3):1277–1289, 1979.

[7] K. H. Hoffmann, J. M. Burzler, and S. Schubert. Endoreversible thermodynamics. *J. Non-Equilib. Thermodyn.*, 22(4):311–355, 1997.

[8] K. H. Hoffmann, J. Burzler, A. Fischer, S. Schubert, and S. Markus. Optimal process paths for endoreversible systems. *J. Non-Equilib. Thermodyn.*, 28(3):233–268, 2003.

[9] J. Burzler. *Performance Optima for Endoreversible Systems*. Dissertation, Technische Universiät Chemnitz, 2002.

[10] A. de Vos. *Endoreversible Thermodynamics of Solar Energy Conversion*. Oxford University Press, Oxford, 1992.

[11] J. M. Gordon and Mahmoud Huleihil. On optimizing maximum-power heat engines. *J. Appl. Phys.*, 69(1):1–7, 1991.

[12] M. Mozurkewich and R. Stephen Berry. Optimal paths for thermodynamic systems: The ideal otto cycle. *J. Appl. Phys.*, 53(1):34–42, 1982.

[13] J. M. Burzler, P. Blaudeck, and K. H. Hoffmann. Optimal piston paths for diesel engines. In Stanislaw Sieniutycz and Alexis De Vos, editors, *Thermodynamics of Energy Conversion and Transport*, pages 173–198. Springer Verlag, New York Berlin Heidelberg, 2000.

[14] A. Bejan. *Entropy Generation Minimization*. CRC Press Inc., Boca Raton, FL, 1996.

[15] A. Bejan. *Advanced Engineering Thermodynamics*. John Wiley and Sons, Inc., 1997.

[16] V. Badescu. On the theoretical maximum efficiency of solar-radiation utilization. *Energy*, 14(9):571–573, 1989.

[17] A. de Vos and H. Pauwels. On the thermodynamic limit of photovoltaic energy conversion. *Appl. Phys.*, 25:119–125, 1981.

[18] M. J. Ondrechen, R. S. Berry, and B. Andresen. Thermodynamics in finite time: A chemically driven engine. *J. Chem. Phys.*, 72(9):5118–5124, 1980.

[19] M. J. Ondrechen, B. Andresen, and R. S. Berry. Thermodynamics in finite time: Processes with temperature-dependent chemical reactions. *J. Chem. Phys.*, 73(11):5838–5843, 1980.

[20] O. C. Mullins and R. S. Berry. Minimization of entropy production in distillation. *J. Phys. Chem.*, 88(4):723–728, 1984.

[21] D. Brown. Simulations of equal thermodynamic distance distillation columns for regular solutions. master thesis, San Diego State University, San Diego, 1998.

[22] P. Salamon and J. D. Nulton. The geometry of separation processes: A horse-carrot theorem for steady flow systems. *Europhys. Lett.*, 42(5):571–576, 1998.

[23] S. Weiss, editor. *Thermisches Trennen*. Deutscher Verlag für Grundstoffindustrie, Stuttgart, 1996.

[24] G. M. de Koeijer, S. Kjelstrup, H. J. van der Kooi, B. Groß, K. F. Knoche, and T. R. Andersen. Positioning heat exchangers in binary tray distillation using isoforce operation. In M. Ishida, editor, *Proceedings of ECOS'99*, pages 471–476, 1999.

[25] G. de Koeijer and S. Kjelstrup. Minimizing entropy production rate in binary tray distillation. *Int. J. Applied Thermodynamics*, 3(3):105–110, 2000.

[26] C. J. King. *Separation Processes*. McGraw-Hill, New York, 1971.

[27] B. Andresen and P. Salamon. Distillation by thermodynamic geometry. In S. Sieniutycz and A. De Vos, editors, *Thermodynamics of Energy Conversion an Transport*, chapter 12, pages 319–331. Springer, New York, 2000.

[28] Z. Fonyo. Thermodynamic analysis of rectification I. Reversible model of rectification. *Int. Chemical Engng.*, 14(1):18–27, 1974.

[29] Z. Fonyo. Thermodynamic analysis of rectification II. Finite cascade models. *Int. Chemical Engng.*, 14(2):203–210, 1974.

[30] R. Rivero. *L'analyse d'exergie: Application à la Distillation et aux Pompes à Chaleur à Absorption*. Phd thesis, Institut National Polytechnique de Lorraine, Nancy, France, 1993.

[31] R. Rivero and P. Le Goff. Heat pumps with diabatic distillation. *Int. J. Refrigeration*, 23:26–30, 2000. in French.

[32] R. Rivero. Exergy simulation and optimization of adiabatic and diabatic binary distillation. *Energy*, 26(6):561–593, 2001.

[33] S. Kjelstrup-Ratkje, E. Sauar, E. Hansen, K. M. Lien, and B. Hafskjold. Analysis of entropy production rates for design of distillation columns. *Ind. Eng. Chem. Res.*, 34:3001–3007, 1995.

[34] E. Sauar, R. Rivero, S. Kjelstrup, and K. M. Lien. Diabatic column optimization compared to isoforce columns. *Energy Conversion and Management*, 38:1777–1783, 1997.

[35] G. de Koeijer, S. Kjelstrup, P. Salamon, G. Siragusa, M. Schaller, and K. H. Hoffmann. Comparison of entropy production rate minimization methods for binary diabatic tray distillation. In A. Öztürk and Y. A. Gögüs, editors, *Proceedings of ECOS 2001*, pages 667–677, Istanbul, 2001.

[36] E. Sauar, S. Siragusa, and B. Andresen. Equal thermodynamic distance and equipartition of forces applied to binary distillation. *J. Phys. Chem. A*, 105(11):2312–2320, 2001.

[37] S. Kjelstrup, D. Bedeaux, and E. Sauar. Minimum entropy production by equipartition of forces in irreversible thermodynamics. *Ind. Eng. Chem. Res.*, 39(11):4434–4436, 2000.

[38] D. Bedeaux, F. Standaert, K. Hemmes, and S. Kjelstrup. Optimization of processes by equipartition. *J. Non-Equilib. Thermodyn.*, 24(3):242–259, 1999.

[39] D. Tondeur and E. Kvaalen. Equipartition of entropy production, an optimization criterion for transfer and separation processes. *Ind. Eng. Chem. Res.*, 26:50–56, 1987.

[40] A. de Vos and B. Desoete. Equipartition principles in finite-time thermodynamics. *J. Non-Equilib. Thermodyn.*, 25:1–13, 2000.

[41] P. Salamon, J. D. Nulton, G. Siragusa, A. Limon, D. Bedeaux, and S. Kjelstrup. A simple example of control to minimize entropy production. *J. Non-Equilib. Thermodyn.*, 27(1):45–55, 2002.

[42] M. Schaller, K. H. Hoffmann, G. Siragusa, P. Salamon, and B. Andresen. Numerically optimized performance of diabatic distillation columns. *Comput. Chem. Eng.*, 25(11–12):1537–1548, 2001.

[43] G. N. Lewis and M. Randall. *Thermodynamics*. McGraw-Hill, New York, 1961.

[44] J. Nulton, P. Salamon, Bjarne Andresen, and Qi Anmin. Quasistatic processes as step equilibrations. *J. Chem. Phys.*, 83(1):334–338, 1985.

[45] J. S. Rowlinson. *Liquids and Liquid Mixtures*. Plenum Press, New York, 1969.

[46] M. J. D. Powell. An effficient method for finding the minimum of a function of several variables without calculating derivatives. *The Computer Journal*, 7(2):155–162, 1964.

[47] J. D. Nulton and P. Salamon. Optimality in multi-stage operations with asymptotically vanishing cost. submitted to *J. Non-Equilib. Thermodyn.*, 2002.

[48] M. Schaller, K. H. Hoffmann, R. Rivero, B. Andresen, and P. Salamon. The influence of heat transfer irreversibilities on the optimal performance of diabatic distillation clumns. *J. Non-Equilib. Thermodyn.*, 27(3):257–269, 2002.

[49] E. S. Jimenez, P. Salamon, R. Rivero, C. Rendon, K. H. Hoffmann, and M. Schaller. Simulation based optimization of a diabatic distillation column. In N. Houbak, B. Elmegaard, B. Qvale, and M. Moran, editors, *Proceedings of ECOS 2003*, Lyngby,Denmark, 2003. IKON.

[50] E. S. Jimenez, P. Salamon, R. Rivero, K. H. Rendon, C. snd Hoffmann, and M. Schaller. Optimization of a diabatic distillation column with sequential heat exchangers. *Ind. Eng. Chem. Res.*, 43(23):7566–7571, 2004.

[51] P. Jimenez, E. S. and Salamon, R. Rivero, C. Rendon, and K. H. Hoffmann. Optimal allocation of heat exchanger inventory in a serial type diabatic distillation column. In R. Rivero, L. Monroy, R. Pulido, and G. Tstatsaronis, editors, *Proceedings of ECOS 2004*, pages 179–187, Mexico, 2004. IMP.

[52] G. De Koeijer, A. Rosjorde, and S. Kjelstrup. Distribution of heat exchange in optimum diabatic distillation columns. *Energy*, 29(12–15):2425–2440, 2004.

[53] G. De Koeijer and R. Rivero. Entropy production and exergy loss in experimental distillation columns. *Chem. Eng. Sci.*, 58(8):1587–1597, 2003.

[54] R. S. H. Mah, J. J. Nicholson, and R. B. Wodnik. Distillation with secondary reflux and vaporization: A comparative evaluation. *AIChE Journal*, 23(5):651–658, 1977.

[55] W. H. Press, S. A. Teukolsky, W. T. Vetterling, and B. P. Flannery. *Numerical Recipes in C*. Cambridge University Press, Cambridge, 2nd edition, 1992.

[56] R. P. Brent. *Algorithms for Minimization without Derivatives*. Prentice-Hall, Englewood Cliffs (NJ), 1973.

[57] J. A. Nelder and R. A. Mead. A simplex method for function minimization. *Computer Journal*, 7:308–313, 1965.

List of Figures and Tables

Figures

Tables

Zusammenfassung

Konventionelle Destillation ist ein weit verbreitetes, jedoch energieintensives und thermodynamisch ineffizientes thermisches Trennverfahren. In gewöhnlichen Destillationskolonnen wird Wärme nur am Verdampfer zugeführt, und nur am Kondensator entzogen. Die damit verbundene hohe Entropieproduktion (= Exergieverlust) kann erheblich reduziert werden, indem die Wärmezufuhr und -abfuhr auch innerhalb der Destillationkolonne an den Siebböden erfolgt. Dieses Konzept wird als diabatische Destillation bezeichnet. Die vorliegende Arbeit beschäftigt sich mit der numerischen Bestimmung der minimalen Entropieproduktion für verschiedene Modellsysteme zur diabatischen Destillation von idealen binären Gemischen.

Ausgehend von den Zustandsgleichungen für ein ideales binäres Gemisch werden die Bilanzgleichungen für die Wärme und Entropie für jeden Siebboden aufgestellt, woraus sich die Entropieproduktion des Gesamtsystems ergibt. Es folgt eine kurze Einführung in die Theorie der Equal Thermodynamic Distance (ETD). Diese ist asymptotisch in der Anzahl der Siebböden, und benutzt eine thermodynamischen Metrik basierend auf der Entropiezustandsfunktion des zu trennenden Gemischs. Aus der ETD-Theorie wird eine untere Schranke für die Entropieproduktion gewonnen (Horse-Carrot-Theorem).

Die erste numerische Untersuchung beschränkt sich auf die Entropieproduktion im Inneren der Destillationskolonne, ohne die Irreversibilität des Wärmeaustauschs mit der Umgebung mit einzubeziehen. Es wird eine ideale Benzol/Toluol-Mischung mit drei verschiedenen Reinheitsvorgaben betrachtet. Die Entropieproduktion der diabatischen Kolonne wird mittels Powell-Verfahren minimiert, ebenso wird die Entropieproduktion einer konventionellen Kolonne als Minimierungsproblem definiert. Die Bodentemperaturen sind hierbei die Kontrollvariablen. Zusätzlich wird sowohl die Entropieproduktion nach der ETD-Theorie, als auch die Horse-Carrot-Schranke berechnet.

Die Darstellung der Entropieproduktion in Abhängigkeit der Bodenanzahl zeigt eine erhebliche Reduktion der Entropieproduktion für optimierte diabatische Kolonnen mit vielen Böden gegenüber einer konventionellen adiabatischen Kolonne. Zum Beispiel verringert sich die Entropieproduktion um fast 80% für eine diabatische Kolonne mit 70 Böden und 99% reinem Destillat. Für kürzere Kolonnen fällt die Reduktion geringer aus, es zeigen sich auch signifikante Abweichungen zwischen numerischem Optimum und asymptotischer ETD-Theorie. Die optimalen Temperatur- und Konzentrationsprofil einer optimalen diabatischen Kolonne zeigen einen gleich-

mäßigeren Anstieg innerhalb der Kolonne, ebenso verteilt sich die Entropieproduktion gleichmäßiger auf alle Böden als im adiabatischen Fall. In einer optimierten Kolonne verringert sich die Heizlast am Verdampfer um bis zu zwei Drittel, die Kühllast am Kondensator reduziert sich um bis zur Hälfte. Bei langen diabatischen Kolonnen sind die zusätzlichen Heiz- und Kühlleistungen ungefähr für alle Böden gleich groß.

In das zweite Modell wird die Irreversibilität des Wärmeaustauschs mit der Umgebung mit einbezogen, wodurch die Entropieproduktion nicht mehr mit der Zulaufrate skaliert. Der Wärmeaustausch wird sowohl mit einem linearen Newton-Gesetz, als auch durch ein inverses Fourier-Gesetz beschrieben. Es wird ein Parameter eingeführt, der das Verhältnis von Zulaufrate und Wärmetransport beschreibt. Für kleine Werte dieses Parameters unterscheiden sich die optimalen Wärmelastprofile nur unwesentlich von der optimalen Lösung für den Fall ohne Irreversibilitäten. Für große Werte diese Parameters dominiert die Entropieproduktion bedingt durch Wärmeaustausch mit der Umgebung. Die optimalen Wärmelastprofile werden zunehmend flacher. Für industriell relevante Werte des Zulaufrate-Wärmetransport-Parameters ist die minimale Entropieproduktion der optimierten Kolonne nur ein Bruchteil der einer konventionellen Kolonne. Mit zunehmender Länge der Kolonne steigt der Anteil der durch die Wärmetauscher bedingten Entropieproduktion.

Eine spezielle Implementierung einer diabatischen Kolonne benutzt einen einzigen Kühlkreislauf mit seriell angeordneten Wärmetauschern für alle Böden oberhalb des Zulaufbodens, und einen einzigen Heizkreiskauf mit seriell angeordneten Wärmetauschern für alle Böden unterhalb des Zulaufbodens. Dadurch reduziert sich die Anzahl der Kontrollvariablen auf die Eintrittstemperaturen und die Massenstromraten der Wärmeträgerfluide in den beiden Kreisläufen. Die Minimierung der Entropieproduktion für diese Anordnung mit den bisher verwendeten Standardmethoden stößt jedoch auf Konvergenzprobleme. Dieses Problem wird durch Anwendung eines heuristischen pseudodynamischen Algorithmus auf das Temperaturprofil innerhalb der Kolonne umgangen. Trotz der drastischen Reduktion der Anzahl von Kontrollvariablen unterscheiden sich die optimalen Betriebsprofile nur unwesentlich von denen einer diabatischen Kolonne mit unabhängig voneinander kontrollierten Bodentemparaturn. Auch ist für letztgenannten Fall die minimale Entropieproduktion nur wenig niedriger als für eine Kolonne mit seriellen Wärmetauschern. Diese Eigenschaft und die potentiell einfache technische Umsetzung machen die Anordnung mit sequentiellen Wärmetauscher für Anwendungen besonders interessant.

Selbständigkeitserklärung gemäß Promotionsordnung §6

Ich erkläre, dass ich die vorliegende Arbeit selbstständig und nur unter Verwendung der angegebenen Literatur und Hilfsmittel angefertigt habe.

Ich erkläre, nicht bereits früher oder gleichzeitig bei anderen Hochschulen oder dieser Universität ein Promotionsverfahren beantragt zu haben.

Ich erkläre, obige Angaben wahrheitsgemäß gemacht zu haben und erkenne die Promotionsordnung der Fakultät für Naturwissenschaften der Technischen Universität Chemnitz vom 10. Oktober 2001 an.

Chemnitz, den 4. Mai 2007 Markus Schaller

Lebenslauf

Markus Schaller
Geboren am 19. Juni 1973 in Vorau (Österreich)

Schule und Wehrdienst

06.1991	Allgemeine Hochschulreife, Graz
02.1998 – 10.1998	Wehrdienst, Kaserne Zeltweg

Universität

10.1991 – 11.1997	Diplomstudium Technische Physik, TU Graz
10.1995 – 06.1996	Auslandsstudium, Strathclyde University, Glasgow
10.1996 – 09.1997	Diplomarbeit: Theory, Simulation and Optimization of Transparent Insulation Materials with Honeycomb Structure
10.1997	Abschluss: Dipl.-Ing.
11.1998 – 10.2001	Doktorand im DFG-Graduiertenkolleg "Regenerative Energiequellen", TU Chemnitz

Berufliche Erfahrungen

11.2001 – 08.2002	Wissenschaftlicher Mitarbeiter, Professur für Computerphysik, TU Chemnitz

Wissenschaftliche Fortbildung

- Workshops, Telluride Summer Research Center, Telluride, USA
  - Thermodynamics of Distillation, Juli 1999
  - Optimality in Staged Unit Operations, August 2000
- Onsager Workshop, Leiden, Niederlande, März 2000
- ECOS '01 Conference, Istanbul, Türkei, Juli 2001

Publikationen

Artikel in Fachzeitschriften

M. Schaller, K. H. Hoffmann, G. Siragusa, P. Salamon, and B. Andresen. Numerically Optimized Performance of Diabatic Distillation Columns. Computers & Chemical Engineering, 25 (11-12), 1537-1548, 2001.

M. Schaller, K. H. Hoffmann, R. Rivero, B. Andresen, and P. Salamon. The Influence of Heat Transfer Irreversibilities on the Optimal Performance of Diabatic Distillation Columns. Journal of Non-Equilibrium Thermodynamics, 27(3), 257-269, 2002.

G. M. de Koeijer, S. Kjelstrup, P. Salamon, G. Siragusa, M. Schaller, and K. H. Hoffmann. Comparison of Entropy Production Rate Minimization Methods for Binary Diabatic Distillation. Industrial & Engineering Chemistry Research, 41(23), 5826-5834, 2002.

K. H. Hoffmann, J. Burzler, A. Fischer, M. Schaller and S. Schubert. Optimal Process Paths for Endoreversible Systems. Journal of Non-Equilibrium Thermodynamics, 28(3), 233-268, 2003.

E. S. Jimenez, P. Salamon, R. Rivero, C. Rendon, K. H. Hoffmann, M. Schaller, and B. Andresen. Optimization of a Diabatic Distillation Column with Sequential Heat Exchangers. Industrial & Engineering Chemistry Research, 43(23), 7566-7571, 2004.

Konferenzbeiträge

G. M. de Koier, S. Kjelstrup, P. Salamon, G. Siragusa, M. Schaller, and K. H. Hoffmann, Comparison of Entropy Production Rate Minimization Methods for Binary Tray Distillation Columns, In A. Ozturk, editor, Proceedings of ECOS 2001, Istanbul, Turkey, 2001.

E. S. Jimenez, P. Salamon, R. Rivero, C. Rendon, K. H. Hoffmann and M. Schaller, Simulation Based Optimization of a Diabatic Distillation Column, In N. Houbak, B. Elmegaard, B. Qvale, and M. Moran, editors, Proceedings of ECOS 2003, Lyngby, Denmark, 2003.